Biochar Metal Sorption and Effect on Microbial Sulfate Reduction

A Thesis
SUBMITTED TO THE FACULTY OF THE
UNIVERSITY OF MINNESOTA
BY

Kipp Sande

IN PARTIAL FULFILLMENT OF THE
REQUIERMENTS
FOR THE DEGREE OF
MASTER OF SCIENCE

Sebastian Behrens

November 2016

Acknowledgements

This research was made possible through funding provided by the MnDRIVE initiative and the Legislative-Citizen Commission on Minnesota Resources (LCCMR). Furthermore, I would like to thank everyone who helped me along the way. In particular, I would like to extend a special thank you to Jovan Popovich for all the help with setting up experiments, Zhe Du for his qPCR work, Eduardo Moreno for his insights into sorption methods, Lee Krumholz for providing the strain of bacteria used, and my committee members Kurt Spokas, Paige Novak, and Sebastian Behrens. I would especially like to thank my advisor Sebastian Behrens for all the help and guidance he has provided along the way. Thank you!

Abstract

Biochar is a stabilized, recalcitrant carbon compound, created when biomass is heated to temperatures between 300-1000°C, under low oxygen concentrations. It can be produced from a variety of biomass feedstock, such as agricultural residues, wood chips, and manure. Recently, biochars have found several applications in environmental remediation. This study evaluated the effect of biochar on microbial sulfate reduction in cell suspension assays and batch growth experiments, as well as the potential of biochar to remove heavy metals from aqueous solution. Irrespective of dosage (0.5 – 10 g/L), biochar increased the extent of sulfate reduction by *Desulfovibrio alaskensis* G20 up to 4-fold in suspension assays. Batch growth experiments demonstrated that biochar concentrations up to 10 g/L have no inhibitory effects on microbial sulfate reduction and cell growth. We further compared the sorptive properties of different biochars for copper and nickel. Biochars were pyrolyzed in the presence of magnesium hydroxide ($Mg(OH)_2$) or magnesium chloride ($MgCl_2$) and sorption isotherms for copper and nickel were compared to unmodified biochar. Copper and nickel sorption capacities were greatly improved for the magnesium-enhanced biochars, indicating that biochar mineral supplementation can increase the efficiency of metal adsorption and removal from solution. Ongoing research under this theme aims at the development of a biochar-mineral composite material that promotes biological sulfate reduction and heavy metal adsorption in order to provide an efficient, low-cost, environmentally-friendly absorbent material that can be used for mine water treatment in bioreactors and/or permeable reactive barriers.

Table of Contents

List of Tables

List of Figures

Introduction

Ferrous and non-ferrous mining play a crucial role in Minnesota's economy. It is estimated that by 2016, mining activities may contribute nearly $5 billion in wages, rents, interest, and profits to Minnesota's economy (Bureau of Business and Economic Research 2012). The possible expansion of mining activities in northeastern Minnesota, particularly non-ferrous sulfide mining, has met resistance from certain public organizations (Minnesota DNR 2013; Barber, et al. 2014). These public organizations fear that sulfide mining will cause damage to the environment due to runoff contaminated with sulfate and metals from these new mine sites. The state of Minnesota is currently facing the challenge to balance the economic gains of mining with the potential adverse environmental effects of increased mining activity in the northeast. With mining playing an important role in Minnesota's economy, finding safe, effective, and efficient ways to treat and remediate mine wastewater is essential.

Sulfide mining has a long history of contaminated mine drainage leading to environmental harm due to the fact that reduced sulfide minerals unearthed during mining are oxidized when exposed to oxygenated surface water (Robb & Robinson, 1995). Oxidation of these sulfide minerals produces sulfuric acid. This sulfuric acid production reduces pH values in the mine drainage, hence the term acid mine drainage (AMD) (Nordstrom, 2011). Furthermore, AMD often contains toxic metals such as copper, cadmium, lead, and nickel (Nordstrom, 2011). This leads to a need to remediate AMD before it can be received by the surrounding environment.

AMD is generated due to the fact that coal and metallic ore deposits are often found in the presence of sulfide minerals (Bigham & Nordstrom, 2000; Evangelou & Zhang,

1995). The simplified equation below shows the oxidation of pyrite in the presence of oxygen, leading to AMD formation in surface waters (Johnson & Hallberg, 2005).

Equation 1

$$4FeS_2 + 15O_2 + 14H_2O \rightarrow 4Fe(OH)_3 + 8SO_4^{2-} + 16H^+$$

As can be seen from Equation 1, the oxidation of these sulfidic minerals can lead to the production of sulfuric acid. This sulfuric acid production can lead to extremely low pH values (pH 0-5) in AMD. Furthermore, the acidic nature of these waste streams can subsequently mobilize toxic heavy metals, such as copper and cadmium, that are often found in the presence of sulfide ore (Nordstrom, 2011). These mobilized heavy metals can have widespread ecological affects, such as reduced biodiversity, in the receiving environment (Johnson & Hallberg, 2005). Furthermore, these heavy metals and low pH values can also inhibit sulfate reducing bacteria that produce sulfide, which is extremely insoluble with many heavy metals.

While pH values in Minnesota AMD generally only reach minimums of around four to five due to the carbonate mineral content of the rocks found in the region, there is an additional concern specific to northern Minnesota (Lapakko and Antonson, 2012). This concern is the increased concentration of sulfate (due to sulfide mineral oxidation) in mine drainage (MD) and subsequent sulfide production in watersheds containing lakes and rivers supporting wild rice that receive said MD. While sulfate is not directly toxic to wild rice plants, if it is reduced to sulfide by sulfate reducing bacteria in sediment supporting the roots of wild rice, it can have inhibitor effects (MPCA, 2015). With wild rice being an important part of Minnesota's heritage, elevated sulfate concentrations (100's to 1000's of milligrams per liter) in MD are particularly significant. This leads to the need to find reliable and efficient sulfate removal techniques that can be applied to MD.

Technologies relating to remediating AMD can be grouped into two categories, abiotic and biological (see Figure 1 below). Biological treatment, such as wetland treatment or sulfidogenic bioreactors, depends on biological activity, while abiotic treatment, such as limestone drains, does not (Johnson & Hallberg, 2005). Remediation technologies can be further subdivided into passive and active systems. Active systems generally require equipment (such as pumps and tanks), continuous maintenance, and operational oversight to achieve remediation target levels (Trumm, 2010). Passive systems rely on natural processes (e.g. physical, biological, geochemical) to remediate AMD. Being that precise engineered controls can be put in place to obtain a specific water quality during active treatment, active treatment technologies generally lead to more reliable remediation of AMD. The reliability of active treatment makes these methods attractive during active mining when large quantities of water need to be processed (Caraballo, Macias, Rotting, Nieto, & Ayora, 2011). Nevertheless, active treatment is often more labor intensive and expensive than passive treatment, due to the high initial cost of manufacturing the system and the continued cost of operation and maintenance. This in turn can make a passive treatment method (when possible) more attractive once a mine is abandoned and continued mitigation cost is to be minimalized (Trumm, 2010).

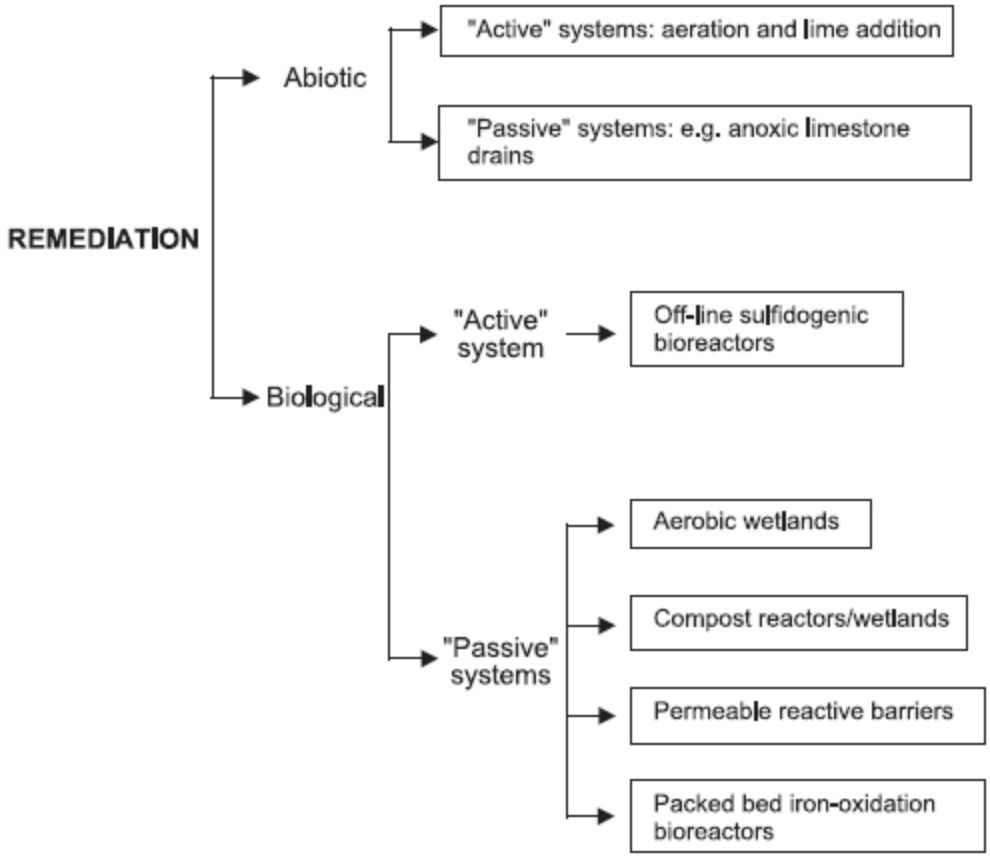

Figure 1: Remediation technologies for AMD (Johnson & Hallberg, 2005).

Remediation of AMD through the use of biochar has received considerable attention due to its ability to sequester various metals in solution and because of its low manufacturing cost (Ahmad et al., 2014; Fellet, Marchiol, Delle Vedove, & Peressotti, 2011). Biochar is the carbonaceous product formed during the heating of biomass under oxygen limited conditions (pyrolysis) (Ahmad et al., 2014; Beesley et al., 2011). Biochar, which consists primarily of carbon, oxygen, and hydrogen, can generally be characterized by a number of unique surface properties (Ennis, Evans, Islam, Ralebitso-Senior, & Senior, 2012). The most significant of these properties includes a large surface area, an abundant array of surface functional groups (hydroxyls, carbonyls, carboxyls), a porous surface

morphology, and an alkaline pH (Ahmad et al., 2014; Tan et al., 2015). It should be noted that acidic biochar is also a possible product during pyrolysis (Ahmad et al., 2014; Sun et al., 2014).

This pyrolysis of biomass results in a stable, recalcitrant, and carbon rich material (Ennis et al., 2012; Lehmann et al., 2011b). This stable material, along with its other unique properties, allows for multiple different uses. Current research has focused on utilizing biochar to sequester CO_2 to help mitigate climate change, as a possible material to be used in supercapacitors, and as a soil amendment to increase soil productivity while simultaneously decreasing CH_4 and N_2O emissions. Recent applications, however, have begun exploring biochar as a way to immobilize contaminants (organic and inorganic) from both soils and aqueous solutions (Ahmad et al., 2014; Ennis et al., 2012; Lehmann et al., 2011a). Furthermore, the production of biochar is often seen as a renewable and cost-effective alternative to traditional sorptive materials such as activated carbon. This is due to the fact that biochar can be produced from abundant, inexpensive, and/or undesired biomass to lower the overall production cost (Babel & Kurniawan, 2004; Nomanbhay & Palanisamy, 2005).

The production of biochar relies on the relatively simple process of pyrolysis. Multiple variables, both in the biomass used and in the pyrolysis parameters, however, have large impacts on the properties, such as surface area, pore volume, and surface function groups, of the end product. These variables include (but are not limited to) the type of biomass used (e.g. manure versus woodchips), pyrolysis temperature, pyrolysis time, and production method (Ennis et al., 2012; Sun et al., 2014). Generally, as pyrolysis temperature is increased, the carbon content and surface area of the product will increase.

In addition, as pyrolysis temperature is increased, the oxygen content and product yield is decreased (Y. X. Han, Boateng, Qi, Lima, & Chang, 2013; Sun et al., 2014). Thus, based on the circumstances for which the pyrogenic carbon is to be used, pyrolysis conditions and biomass can be chosen to optimize the end product for a specific application.

Recently, research has been devoted to creating "engineered" biochar. This field of study focuses on the chemical modification of biochar so as to maximize a certain functional property. These chemical modifications include (but are not limited to) acid/base treatment, chemical precipitation, and chemical impregnation (Fang, Zhang, Li, Jiang, & Wang, 2014; Z. T. Han et al., 2015; Li et al., 2014). Various modification processes rely on either pretreatment of the biomass before pyrolysis, or post treatment of the produced pyrogenic carbon. Pretreatment generally involves soaking the biomass before pyrolysis in a chemical solution to obtain uptake of a desired chemical. Post treatment involves modification following the pyrolysis of the biomass. Most modifications utilizing post treatment use acid/base treatment or chemical precipitation to obtain the desired modification. For example, in an article by Chen et al., biochar impregnated with magnetite was created by pretreating the biomass in a solution of ferrous and ferric iron. This magnetite modified pyrogenic carbon was found to exhibit magnetic properties such that it could be separated from aqueous solutions utilizing a magnet, leading to the possibility of easy separation from solution following sorption of various contaminants (Chen, Chen, & Lv, 2011). In another study, chitosan was loaded onto the surface of biochar (post treatment) derived from oil palm shell for the removal of chromium from wastewater (Nomanbhay & Palanisamy, 2005). This modification resulted in a large sorption capacity

for chromium with the added benefit that the sorbent could be reused following regeneration by sodium hydroxide (Nomanbhay & Palanisamy, 2005).

In addition, biochar has been shown to have positive impacts on microorganism populations. This is due to the fact that biochar contains macropores (>200 nm) in which microorganisms can live, creating micro-niches for specific bacteria while also protecting them from predation (Gul, Whalen, Thomas, Sachdeva, & Deng, 2015). Biochar can also increase microbial biomass by increasing soil water retention, nutrient and organic matter availability (through sorption and/or release), soil pH, and by sorbing toxins (Beesley et al., 2011; Lehmann et al., 2011a). Furthermore, biochar has been implicated as an electron shuttle in various biological systems due to its highly aromatic carbon structure and redox active surface functional groups. Electron shuttling by both solid-phase and soluble humic substances (which are high molecular weight redox active organics ubiquitous in the environment) is already recognized and has been shown to significantly increase redox reactions. In the article by Lovley et al., it was shown that iron(III) oxide reduction by *Geobacter metallireducens* was stimulated by the addition of soluble humic substances (Lovley, Coates, BluntHarris, Phillips, & Woodward, 1996). These humic substances were believed to have mediated the transfer of electrons from the cells to the solid ferric iron (Lovley et al., 1996). Another article by Roden et al. showed that solid-phase humics, which are much more common in soil environments, accelerated iron(III) oxide reduction by both *Geobacter sulfurreducens* and *Shewanella putrefaciens* by possibly acting as a solid-state electron shuttle (Roden et al., 2010).

Biochar, which is also redox active, similar to humic substances, has already been shown to be able to act as an electron shuttle. Kappler et al. shower that biochar was able

to act as an electron shuttle to transfer electrons onto a solid iron(III) (ferrihydrite) electron acceptor from *Shewanella oneidensis* MR-1. In addition, biochar increased the rate of ferrihydrite reduction and extent of reduction (Kappler et al., 2014). In another study performed by Xu et al., *S. oneidensis* MR-1 and biochar were used to test the effect of biochar on hematite reduction (Xu et al., 2016). This study found that biochar increased 240 hour hematite reduction extents by 50-100%, as compared to biochar-free controls (Xu et al., 2016). Biochar has also been implicated as an electron shuttle for the dechlorination of pentachlorophenol (PCP) by *Geobacter sulfurreducens* (Yu, Yuan, Tang, Wang, & Zhou, 2015). In this study, the addition of biochar resulted in an 8-fold increase in PCP degradation after 21 days, as compared to the biochar-free control (Yu et al., 2015). However, how biochar interacts with sulfate reducing bacteria/if it can act as an electron shuttle is currently unknown.

This study attempts to address the following questions and gaps in existing research: 1. Does engineered biochar increase sorption capacities towards heavy metals, in particular, copper and nickel, 2. Can biochar act as an electron donor/acceptor to increase sulfate reduction rates and/or sulfate reducing bacteria (SRB) growth yield 3. Can biochar relieve heavy metal stress from SRB through its sorptive capacity? In this study, engineered $MgCl_2$ and $Mg(OH)_2$ modified biochar are tested for nickel and copper sorption to evaluate if modification resulted in an increase in sorption capacity compared to unmodified biochar. These modified biochars were selected to increase sorption capacity towards heavy metals, due to increased ion exchange capacity and metal surface complexation. Furthermore, *Desulfovibrio alaskensis* G20 was used as a model SRB to test the hypothesis that biochar can act as an electron shuttle during biotic sulfate reduction, and in turn,

stimulate sulfate reduction. *D. alaskensis* is an obligate anaerobe that completely reduces sulfate to sulfide though the oxidation of simple organic molecules (i.e. lactate and formate) (Muyzer & Stams, 2008). No previous study investigating the effect of biochar on microbial sulfate reduction has been performed to date. The last part of this study involves testing the hypothesis of reducing either copper or nickel metal stress in a growing culture of *D. alaskensis* by adding biochar. It is believed that biochar will be able to sorb a certain amount of copper and nickel, reducing the concentration of available metal the bacteria are exposed to. Overall, this study looks to test the effect both the sorptive and redox properties of biochar have on microbial sulfate reduction. This study has direct impacts towards possible passive (such as permeable reactive barriers) or active (such as sulfidogenic bioreactors) remediation technologies regarding AMD through the use of SRB and biochar.

Methods

Chemicals/Materials

All chemicals used were of at least reagent grade (Sigma Aldrich).

Sorption Experiment

-Production of Biochar Composite Materials

Three different biochars were tested for their sorption capacity towards nickel and copper in solution, unmodified Swiss biochar, magnesium hydroxide ($MgOH_2$) modified biochar, and magnesium chloride ($MgCl_2$) modified biochar (Swiss Biochar, Belmont-sur-Lausanne, Switzerland). Engineered biochars were produced by blending waste biomass with metals prior to thermal treatment of the organic material. Biochars were produced from wood chips. Prior to pyrolysis, the wood chips were mixed with magnesium chloride, or magnesium hydroxide. All biochars were produced at 700°C in a PYREG pyrolysis reactor. The prepared biochar-based sorbents were characterized by determining basic physio-chemical properties such as pH, electrical conductivity (EC), metal leaching, and mass losses at pH 3, 5 and in distilled water (DW). The unmodified Swiss biochar was used as a control. In depth elemental composition of the control Swiss biochar can be found in Appendix A: Swiss Biochar Properties. Table 1 and Table 2 below show the above mentioned biochar physio-chemical properties. Before use, each individual biochar was first ground and sieved to obtain a particle size range of 125 to 500 microns. All biochars were ground using a mortar and pestle. The sieve shaker used was a RO-TAP Model RX-29 (W.S. Tyler). Sieving was performed for 20 minutes.

Table 1: Tested biochar properties; ME stands for soluble metal extracts from biochar. N.D. stands for not determined. All reported properties are for unwashed biochar.

Biochar	pH	EC [mS/cm]	Me (pH 3) [mg/g]	Me (pH 5) [mg/g]	ME (DW) [mg/g]
Control	10.35	0.424	N.D.	N.D.	N.D
$MgCl_2$	9.86	1.655	2.374	2.322	2.315
$Mg(OH)_2$	10.48	0.553	1.898	1.880	1.832

Table 2: Tested biochar properties: ML stands for mass lost. All reported properties are for unwashed biochar.

Biochar	ML (pH 3) [%]	ML (pH 5) [%]	ML (DW) [%]
Control	0.185	0.084	0.078
$MgCl_2$	0.458	0.387	0.372
$Mg(OH)_2$	0.561	0.372	0.364

-*Metal Solution Preparation*

Stock solutions containing 1000 mg/L cupric sulfate or nickel sulfate were made in DI water using 250 mL volumetric flasks. Potassium chloride was included in these stock solutions at a concentration of 0.01 M to serve as a background electrolyte. To achieve the appropriate metal concentrations, the stock solution was diluted using 0.01 M potassium chloride containing DI water (dilution solution) so as to not change the background electrolyte concentration. The metal concentrations used to generate the isotherms were chosen to range from 0 to 80 mg/L in 10 mg/L increments. To achieve these final metal concentrations, the appropriate metal stock solution was diluted into the dilution solution. These dilutions were performed in 250 mL volumetric flasks using 10 and 5 mL pipettes to aliquot the metal stock solution. Table 3 below shows the volumes of metal stock solution and dilution solution used to generate the needed metal concentrations.

Table 3: Metal stock solution and dilution solution volumes needed for dilution to needed metal concentrations.

Final Metal Concentration [mg/L]	Volume of Stock Solution Needed [mL]	Volume of Dilution Solution Needed [mL]
0	0	250
10	2.5	247.5
20	5	245
30	7.5	242.5
40	10	240
50	12.5	237.5
60	15	235
70	17.5	232.5
80	20	230

Each solution was then acidified by dropwise addition of 0.5 M hydrochloric acid to a pH of 4.0 ± 0.1.

-Batch Sorption Procedure

A batch sorption technique was used to determine the metal sorption capacity for each biochar. This technique relies on shaking/mixing until equilibrium is established between the sorbent and the sorbate. By measuring the starting concentration and equilibrium concentration of the sorbate, Equation 2 below can be used to determine sorption capacity.

Equation 2:

$$Q = \frac{Ci - Cf}{m/V}$$

Where

- Q = sorption capacity [mg/g]
- Ci = initial sorbate concentration [mg/L]
- Cf = final sorbate concentration [mg/L]
- m = mass of sorbent (biochar) [g]
- V = volume of solution [mL]

In this study, 20 mL of metal solution was added to 50 mL polypropylene falcon tubes containing 10 ± 0.3 mg of the biochar to be tested (United Scientific Supplies Inc.). This resulted in a biochar dose of 0.5 g/L. Tubes containing the biochar/metal mixture were then placed on a rotating inverter for 48 hours (Glas-Col). This rotating inverter completely inverted the falcon tubes at a speed of 45 rotations per minute. To ensure precipitation of the metals did not occur due to the alkalinity of the biochars, tubes were taken off the inverter at certain times during the 48-hour interaction time to have their pH checked and adjusted. pH check and adjustment times were 0.25, 1, 2, 4, 6, 18, 30, 42, 45, 45.5, 46, 46.5, 47, 47.5, and 47.75 hours. 0.01, 0.5, and 0.1 M hydrochloric acid were used to adjust the pH's back down to 4.0 when necessary. The total volume added to adjust the pH of each mixture was tracked throughout and accounted for during final sorption calculations.

After 48 hours of interaction time, each mixture was taken off the inverter, checked for final pH, and then filtered into a clean tube using a 0.2 µm nylon syringe filter (Whatman). Each filtered mixture was then acidified to roughly 2.0 with 50 µL of 0.5 M HCl and stored at room temperature for metal analysis. All runs were performed in triplicate at 25˚ C. The isotherms were then fit with either the Langmuir or the Freundlich model (see Equation 3 and Equation 4 for each model below) using nonlinear regression (Microsoft Excel). The Langmuir model assumes monolayer adsorption with all binding sites being identical, while the Freundlich model does not assume monolayer adsorption, and also accounts for different binding sites having different energy (Limousin et al., 2007). Please see Limousin et al., 2007 for a complete review on these isotherm models. An example of how the nonlinear regression was performed can be seen in Appendix B: Nonlinear Regression Example for Nickel Sorption onto $MgCl_2$ Modified Biochar.

Equation 3: Langmuir Isotherm

$$Q = \frac{Qm * KL * Cf}{(1 + KL * Cf)}$$

Where

- Q = sorption capacity [mg/g]
- Qm = maximum sorption capacity [mg/g]
- Cf = initial sorbate concentration [mg/L]
- KL = Constant [L/mg]

Equation 4: Freundlich Isotherm

$$Q = F * Cf^{n}$$

Where

- Q = sorption capacity [mg/g]
- F = Freundlich constant [L/g]
- Cf = final sorbate concentration [mg/L]
- n = constant [ ]

-Flame Atomic Absorption Spectroscopy Analysis (FAAS)

Initial and final metal concentrations in solution were measured using FAAS with acetylene as the fuel and ultra-pure air as the oxidant (Perkin Elmer AAS 100). 1000 mg/L metal stock standard calibration solutions were made in 1% nitric acid solution. All calibration solutions were freshly made by diluting into DI water. Copper concentrations were measured at a wavelength and slit of 324.8 and 0.7 nm, respectively. Nickel concentrations were measured at a wavelength and slit of 352.5 and 0.2 nm, respectively.

These FAAS settings resulted in linear ranges from 0 to 20 mg/L and 40 mg/L for copper and nickel, respectively. These linear ranges made it necessary to dilute the samples from the sorption experiments. The dilution factors used for each different metal concentration are shown in Table 4 and Table 5 below. Initial metal concentrations were also determined using the same dilution factor. Initial metal concentrations were determined by performing FAAS on the diluted metal solutions before biochar addition.

Table 4: Copper dilutions used for FAAS analysis. ND = no dilution.

Copper Concentration [mg/L]	Dilution	Dilution Factor
0	N.D.	1
10	N.D.	1
20	1:1	2
30	1:1	2
40	1:2	3
50	1:2	3
60	1:3	4
70	1:3	4
80	1:4	5

Table 5: Nickel dilutions used for FAAS analysis.

Nickel Concentration [mg/L]	Dilution	Dilution Factor
0	N.D.	1
10	N.D.	1
20	N.D.	1
30	N.D.	1
40	1:1	2
50	1:1	2
60	1:1	2
70	1:2	3
80	1:2	3

Growth Curve/Cell Suspension Experiments

-Desulfovibrio alaskensis G20 Media

D. alaskensis G20 was chosen to be used as the model SRB for all experiments and was obtained from the Lee Krumholz's lab at Oklahoma University. The media used for cultivation, which was an adaptation from (Brandis & Thauer, 1981; Rapp & Wall, 1987), contained lactate as the electron donor and carbon source, and sulfate as the electron acceptor (from here on referred to as LS media) (Brandis & Thauer, 1981; Rapp & Wall, 1987). The complete recipe for the LS media used for cultivation in these experiments can be seen in Table 6-8.

Table 6: Composition of LS media components (per liter basis).

Compound	**Mass per Liter [g]**
NH_4Cl	1.0698
KH_2PO_4	0.2294
$MgSO_4*7H_20$	1.9718
$CaCl_2*H_20$	0.0882
Na_2SO4	7.102
Na Lactate	6.7214
HEPES	5.9575

Table 7: Composition of LS media vitamin mix (10X) (per liter basis).

Compound	Mass per Liter [mg]
Biotin	20
Folic acid	20
Pyridoxin HCl	100
Thiamine HCl	50
Riboflavin	50
Nicotinic acid	50
DL-Pamtothinic acid	50
B12	1
p-aminobenzoic acid	50
Lipoic acid	50
Choline chloride	2

Table 8: Composition of LS media mineral mix (per liter basis).

Compound	Mass per Liter [g]
*Nitriloacetic acid	12.8
$FeCl_2$*$4H_20$	1
$MnCl_2$*$4H_20$	0.5
$CoCl_2$*$6H_20$	0.3
$ZnCl_2$	0.2
Na_2MoO_4*$2H_20$	0.050
H_3BO_3	0.020

*pH adjusted to 6.5 with NaOH

Briefly, all LS components (Table 6) were weighed and mixed into roughly 900 mL of Milli-Q water. 1 mL of vitamin mix (Table 7) and 12.5 mL of mineral mix (Table 8) were then added to the LS media mixture. The pH of this mixture was then adjusted to 6.8-7.0 with hydrochloric acid. The volume was then brought up to 1 L by addition of Milli-Q water and sterilized by autoclaving (30 minutes at 121˚C). No reducing agents were added.

Instead, the media was placed into an anaerobic glove box (Vacuum Atmospheres Co. Nex Gen) and allowed to degas for 48 hours. The media could then be dispensed into glass serum bottles (Wheaton) and stoppered with blue butyl stoppers within the glove box to maintain anaerobic conditions. These filled serum bottles were then crimped with aluminum crimp caps and autoclaved (30 minutes at 121˚ C) to ensure sterility before use.

-D. alaskensis Growth in the Presence of Biochar

To test the effect of biochar/biochar dose on the growth of *D. alaskensis*, batch growth curves were made by inoculating *D. alaskensis* into LS media containing varying doses of biochar. The biochar doses chosen to be tested were 0.5, 1.0, 5.0, and 10.0 g/L. A control containing no biochar and an abiotic control containing 5.0 g/L biochar but no cells were also included. These batch tests were performed in 100 mL serum bottles (Wheaton). First, biochar was weighed out and placed into the serum bottles. These serum bottles were then covered with aluminum foil and placed inside a gloves box to degas for a minimum of 24 hours. LS media was also prepared and degassed inside a glove box as explained above. After at least 24 hours of degassing time, LS media was measured and put into each serum bottle. This transfer was performed inside the glove box using a pipette (Easypet 3, Eppendorf). The volume taken up by biochar was taken into account when adding LS media to the serum bottles (0.5 g of biochar was determined to displace roughly 2.0 mL of water). 50 mL was determined to be the total volume of each batch growth sample, including a 5% inoculation volume (5 mL) of active log phase growth culture (O.D. 600 of 0.560). All biochar doses were run in triplicate. Table 9 below shows volumes and weights needed for each biochar dose.

Table 9: Masses and volumes of components needed for batch growth experiment.

Sample	Biochar Dose [g/L]	Biochar Added [g]	LS Media Added [mL]	Cells Added [mL of active culture]	Total Volume [mL]
1-1	0.5	0.025	45.0	5.0	50.0
1-2					
1-2					
2-1	1.0	0.05	45.0	5.0	50.0
2-2					
2-3					
3-1	5.0	0.25	44.0	5.0	50.0
3-2					
3-3					
4-1	10.0	0.5	43.0	5.0	50.0
4-2					
4-3					
5-1	0.0	0.0	45.0	5.0	50.0
5-2					
5-3					
6-1	5.0	0.25	44.0	0 (5.0 mL of anoxic and sterile Milliq water added)	50.0
6-2					
6-3					

After addition of the LS media to the serum bottles in the glove box, the serum bottles were then stoppered with blue butyl stoppers to maintain anaerobic conditions. The serum bottles were then taken out of the glove box, crimped, and autoclaved (30 minutes at 121˚ C). After autoclaving, the serum bottles were cooled to roughly 25˚ C. Each serum bottle was then either inoculated with an actively growing culture of *D. alaskensis,* or with anaerobic, sterile Milli-Q water (abiotic control). All inoculations were performed sterilely and anaerobically using a gassing station. These inoculations were then incubated at 30˚ C (Thermo Scientific Heratherm Incubator) and sampled for sulfide, sulfate, lactate, acetate, and cell number (by real-time polymerase chain reaction (qPCR)) at designated times.

-D. alaskensis Metal Inhibition Growth

To test if biochar is able to relieve metal stress through its sorption abilities properties, batch growth of *D. alaskensis* in the presence of either nickel or copper was performed in LS media. This experiment closely resembled the first batch growth experiment that was explained earlier. First, LS media was made as was explained. The pH of this media, however, was adjusted to 6.5 before being autoclaved and placed into an anaerobic glove box for degassing. This lower pH was chosen so as to reduce precipitation of nickel and copper with hydroxide (OH). Next, stock solutions of either nickel or copper were made in Milli-Q water. These metal solutions were put in serum bottles (either 50 or 100 mL volumes depending on the volume of stock solution needed) and degassed in an anaerobic chamber for a minimum of 24 hours. Milli-Q water in a 50 mL serum bottle was also placed into an anaerobic chamber and degassed for 24 hours. 25 mM HEPES buffer solution (pH = 6.5, adjusted with HCl or NaOH) was also made and placed in a 100 mL serum bottle and put into the glove box. This solution was used to wash/resuspend the cells that were to be inoculated for the growth experiment.

Biochar was then weighed out into 50 mL serum bottles so as to have a dose of 1.0 g/L in a total volume of 50 mL. These biochar containing serum bottles were placed in an anaerobic glove box to degas for a minimum of 24 hours. Serum bottles containing no biochar were also placed in an anaerobic glove box. These serum bottles were to be used as controls to test for growth in metal containing LS media with no biochar, and also for a control with just LS media. After degassing, LS media was pipetted into each serum bottle in a series. This was performed within the glove box with a pipette (Easy Pet 3). All serum

bottles (including the metal solutions, Milli-Q bottle, and HEPES solution) were then stoppered within the glove box to ensure anaerobic conditions. These serum bottles were then taken out of the glove box and autoclaved (30 minutes at 121˚ C). After autoclaving and cooling, metal solution and Milli-Q water was added to each serum bottle as appropriate sterilely and anaerobically using a Bunsen burner and gassing station. Table 10 and Table 11 below shows matrices containing volumes and concentrations of solutions added to each triplicate series for both the nickel and copper experiment respectively. Realized nickel and copper concentrations can be found in Appendix E: Initial Copper/Nickel Concentrations and Initial pH in Metal Inhibition Growth Studies.

Table 10: Composition of *D. alaskensis* nickel metal inhibition growth experiment samples.

Sample	Sample Nickel Conc. [mg/L]	Conc. Of Nickel Solution [mg/L]	Nickel Solution Added [mL]	Milli Q Added [mL]	Mass Biochar [g]	Inoculation Solution Added [mL]	LS Media Added [mL]	Final Vol. [mL]
1-1	0	---	0.0	5	0.0000	2.5	42.5	50
1-2	0	---	0.0	5	0.0000	2.5	42.5	50
1-3	0	---	0.0	5	0.0000	2.5	42.5	50
2-1	20	200	5.0	0	0.0500	2.5	42.5	50
2-2	20	200	5.0	0	0.0500	2.5	42.5	50
2-3	20	200	5.0	0	0.0500	2.5	42.5	50
3-1	60	600	5.0	0	0.0500	2.5	42.5	50
3-2	60	600	5.0	0	0.0500	2.5	42.5	50
3-3	60	600	5.0	0	0.0500	2.5	42.5	50
4-1	120	1200	5.0	0	0.0500	2.5	42.5	50
4-2	120	1200	5.0	0	0.0500	2.5	42.5	50
4-3	120	1200	5.0	0	0.0500	2.5	42.5	50
5-1	20	200	5.0	0	0.0000	2.5	42.5	50
5-2	20	200	5.0	0	0.0000	2.5	42.5	50
5-3	20	200	5.0	0	0.0000	2.5	42.5	50
6-1	60	600	5.0	0	0.0000	2.5	42.5	50
6-2	60	600	5.0	0	0.0000	2.5	42.5	50
6-3	60	600	5.0	0	0.0000	2.5	42.5	50
7-1	120	1200	5.0	0	0.0000	2.5	42.5	50
7-2	120	1200	5.0	0	0.0000	2.5	42.5	50
7-3	120	1200	5.0	0	0.0000	2.5	42.5	50
8-1	60	600	5.0	2.5	0.0500	0	42.5	50
8-2	60	600	5.0	2.5	0.0500	0	42.5	50
8-3	60	600	5.0	2.5	0.0500	0	42.5	50

Table 11: Composition of *D. alaskensis* copper metal inhibition growth experiment samples.

Sample	Sample Copper Conc. [mg/L]	Conc. Of Copper Solution [mg/L]	Copper Solution Added	Milli Q Added [mL]	Mass Biochar [g]	Inoculation Solution Added [mL]	LS Media Added [mL]	Final Vol. [mL]
1-1	0.0	---	0.0	5	0.0000	2.5	42.5	50
1-2	0.0	---	0.0	5	0.0000	2.5	42.5	50
1-3	0.0	---	0.0	5	0.0000	2.5	42.5	50
2-1	0.5	5	5.0	0	0.0500	2.5	42.5	50
2-2	0.5	5	5.0	0	0.0500	2.5	42.5	50
2-3	0.5	5	5.0	0	0.0500	2.5	42.5	50
3-1	2.5	25	5.0	0	0.0500	2.5	42.5	50
3-2	2.5	25	5.0	0	0.0500	2.5	42.5	50
3-3	2.5	25	5.0	0	0.0500	2.5	42.5	50
4-1	5.0	50	5.0	0	0.0500	2.5	42.5	50
4-2	5.0	50	5.0	0	0.0500	2.5	42.5	50
4-3	5.0	50	5.0	0	0.0500	2.5	42.5	50
5-1	0.5	5	5.0	0	0.0000	2.5	42.5	50
5-2	0.5	5	5.0	0	0.0000	2.5	42.5	50
5-3	0.5	5	5.0	0	0.0000	2.5	42.5	50
6-1	2.5	25	5.0	0	0.0000	2.5	42.5	50
6-2	2.5	25	5.0	0	0.0000	2.5	42.5	50
6-3	2.5	25	5.0	0	0.0000	2.5	42.5	50
7-1	5.0	50	5.0	0	0.0000	2.5	42.5	50
7-2	5.0	50	5.0	0	0.0000	2.5	42.5	50
7-3	5.0	50	5.0	0	0.0000	2.5	42.5	50
8-1	2.5	25	5.0	2.5	0.0500	0	42.5	50
8-2	2.5	25	5.0	2.5	0.0500	0	42.5	50
8-3	2.5	25	5.0	2.5	0.0500	0	42.5	50
9-1*	1.0	10	5.0	0	0.0500	2.5	42.5	50
9-2*	1.0	10	5.0	0	0.0500	2.5	42.5	50
9-3*	1.0	10	5.0	0	0.0500	2.5	42.5	50
10-1*	1.0	10	5.0	0	0.0000	2.5	42.5	50
10-2*	1.0	10	5.0	0	0.0000	2.5	42.5	50
10-3*	1.0	10	5.0	0	0.0000	2.5	42.5	50

Notes: The samples marked with a * represent another copper metal inhibition growth experiment that took place after the first one. A control series exactly the same as the 1-x series was also included for the second set of experiments.

To create the inoculation solution containing *D. alaskensis*, 65 mL of *D. alaskensis* culture was grown for approximately 96 hours in LS media (pH = 6.5) at 30 degrees C (resultant optical density at 600 nm (O.D. 600) of 0.350). After 96 hours, this culture was spun down in sterile falcon tubes (Corning) at 5000 rpm for 7.5 minutes (Eppendorf Centrifuge 5430R). The culture was first placed in a -15˚ C freezer (Kenmore) for 10

minutes before being spun down to reduce microbial activity. After spinning down, excess solution was poured out so that only the cell pellet remained. This cell pellet was then resuspended in 65 mL of the 25 mM sterile and anaerobic HEPES buffer solution (pH = 6.5). After resuspension, the inoculation solution was then placed back into the HEPES buffer serum bottle and degassed with nitrogen. The liquid part was degassed for 15 minutes, and the headspace for 5 minutes. This was performed using a gassing station. A sterile 0.2 µm syringe filter (Pall Corporation: Acrodisc syringe filter) was attached to the degassing line to ensure sterile nitrogen during degassing. The serum bottle was then stoppered and capped. All work was performed next to a Bunsen burner (Eisco Bunsen burner) to ensure sterile working conditions. Cells were then inoculated into the serum bottles anaerobically using a gassing station. These inoculations were then incubated at 30 degrees C. Samples were then taken at set time points for sulfate concentration and cell number (by qPCR analysis). All treatments were performed in triplicate.

-D. alaskensis Cell Suspension in the Presence of Biochar

To measure the effect biochar has on *D. alaskensis* metabolic activity, resting cell suspensions containing varying doses of biochar were made. The biochar doses chosen to be tested were 0.5, 1.0, 5.0, and 10.0 g/L. A control containing no biochar and abiotic controls containing the chosen biochar doses were also included. These batch tests were performed in 50 mL serum bottles. First, biochar was weighed out and placed into the serum bottles. These serum bottles were then covered with aluminum foil and placed inside a gloves box to degas for a minimum of 24 hours.

Next, 1 M sodium sulfate and 1 M sodium lactate solution were made in Milli-Q water and placed in 100 mL serum bottles. A 30 mM HEPES buffer solution was next made in Milli-Q water and placed in a beaker. These three solutions were then degassed in an anaerobic glove box for a minimum of 24 hours. Following degassing, the appropriate amount of HEPES buffer was added to each serum bottle anaerobically within the glove box using a pipette (Easypet 3). The serum bottles, 1 M sulfate solution, and 1 M lactate solution, were then stoppered, taken out of the anaerobic glove box, crimped, and sterilized by autoclaving on a liquid 30 cycle. The amounts of sulfate, lactate, and HEPES solution added to each serum bottle can be seen in Table 12 below. The sulfate and lactate solutions were added to the biochar/HEPES buffer serum bottles post autoclaving to ensure no chemical interactions between the biochar and sulfate/lactate during the heat cycle. After the solutions were cooled to room temperature following autoclaving, sulfate and lactate solutions were added to the serum bottles, sterilely and anaerobically using a gassing station, to obtain 30 mM sulfate and 50 mM lactate final concentrations in the serum bottles.

Table 12: Composition of *D. alaskensis* cell suspension. BC stands for biochar.

Composition of Serum Bottles	Biochar Added [g]	Bottle Number	Cells Added [mL]	30 mM HEPES Added [mL]	1M Sulfate (30 mM Final) Added [mL]	1M Lactate (50 mM Final) Added [mL]
0.5 g/L BC + Cells + 30 mM Sulfate + 50 mM Lactate	0.0125	1-1	2.5	20.5	0.75	1.25
	0.0125	1-2	2.5	20.5	0.75	1.25
	0.0125	1-3	2.5	20.5	0.75	1.25
1 g/L BC + Cells + 30 mM Sulfate + 50 mM Lactate	0.0250	2-1	2.5	20.5	0.75	1.25
	0.0250	2-2	2.5	20.5	0.75	1.25
	0.0250	2-3	2.5	20.5	0.75	1.25
5 g/L BC + Cells + 30 mM Sulfate + 50 mM Lactate	0.1250	3-1	2.5	20.5	0.75	1.25
	0.1250	3-2	2.5	20.5	0.75	1.25
	0.1250	3-3	2.5	20.5	0.75	1.25
10 g/L BC + Cells + 30 mM Sulfate + 50 mM Lactate	0.2500	4-1	2.5	20.5	0.75	1.25
	0.2500	4-2	2.5	20.5	0.75	1.25
	0.2500	4-3	2.5	20.5	0.75	1.25
Cells + 30 mM Sulfate + 50 mM Lactate	0.0000	5-1	2.5	20.5	0.75	1.25
	0.0000	5-2	2.5	20.5	0.75	1.25
	0.0000	5-3	2.5	20.5	0.75	1.25
0.5 g/L BC + 30 mM Sulfate + 50 mM Lactate (ABIOTIC)	0.0125	6-1	0.0	23	0.75	1.25
	0.0125	6-2	0.0	23	0.75	1.25
	0.0125	6-3	0.0	23	0.75	1.25
1 g/L BC + 30 mM Sulfate + 50 mM Lactate (ABIOTIC)	0.0250	7-1	0.0	23	0.75	1.25
	0.0250	7-2	0.0	23	0.75	1.25
	0.0250	7-3	0.0	23	0.75	1.25
5 g/L BC + 30 mM Sulfate + 50 mM Lactate (ABIOTIC)	0.1250	8-1	0.0	23	0.75	1.25
	0.1250	8-2	0.0	23	0.75	1.25
	0.1250	8-3	0.0	23	0.75	1.25
10 g/L BC + 30 mM Sulfate + 50 mM Lactate (ABIOTIC)	0.2500	9-1	0.0	23	0.75	1.25
	0.2500	9-2	0.0	23	0.75	1.25
	0.2500	9-3	0.0	23	0.75	1.25

To create the cell suspension, 2 L of *D. alaskensis* cells were grown in LS media for approximately 72 hours. Next, the cultures O.D. 600 was taken so as to be able to relate the OD 600 to cell number (based off of former cell counts). The *D. alaskensis* culture was then spun down and resuspended in 30 mM HEPES (pH = 7.0). The resuspension volume was chosen so as to result in a concentration of 2^x10^{10} cells per mL, based off of the original calculated cell number from the OD 600. The cell concentration of 2^x10^{10} cells per mL ensured that when the serum bottles were inoculated, 2^x10^9 cells would be added to each serum bottle. The resuspended inoculation solution was then placed in a serum bottle and degassed as described before. Cells were then inoculated into the serum bottles

anaerobically and sterilely using a gassing station. Sulfate and sulfide were then sampled at set time points for 72 hours.

-*Specific Growth Rate (SGR) Analysis*

SGR was determined by plotting the log of the cell number during exponential growth (0 – 48 hours) to obtain a linear line for the batch growth experiment. The slope of this linear line was then multiplied by 2.303 to get SGR (hr^{-1}). For the copper inhibition SGR, SGR was calculated from when the culture showed growth (based on visual observation) to when sulfate reduction was found to have stopped (based on sulfate data).

Analytics

-*Sulfide Measurements*

Sulfide was measured using the method described by Cord-Ruwisch (Cordruwisch, 1985). This is a spectrometric method that relies on colloidal precipitation of sulfide with copper. Briefly, a copper reagent solution consisting of 50 mM HCl and 5 mM $CuSO_4$ (copper sulfate) was made in Milli-Q water. This solution was then aliquoted out in 0.975 mL volumes into 1.5 mL centrifuge tubes (Eppendorf). Next, a solution of sodium sulfide was made by dissolving Na_2S*9H_20 (sodium sulfide nonahydrate) anoxically into a graduated cylinder containing Milli-Q water. By weighing the graduated cylinder before and after the addition of the sodium sulfide nonahydrate, the concentration of sulfide in solution could be determined. This solution was then serially diluted in 1.5 mL centrifuge tubes so as to be able to develop a standard curve. The concentrations of sulfide used for the generation of the standard curve were 20 mM, 10 mM, 5.0 mM, 2.5 mM, and 1.25 mM.

Before significant degassing of the standard curve solutions occurred, 0.25 mL of standard curve solution was pipetted into a 1.5 mL centrifuge tube containing the copper reagent solution. This mixture was then vigorously shaken by hand for 20 s, poured into a 1.5 mL cuvette, and the absorbance at 480 nm measured on a spectrophotometry (Spectronic 20 Genesys, Spectronic Instruments). This same method was then repeated for each different standard curve solution. A linear plot of the absorbance versus concentration could then be made and used to correlate absorbance to sulfide concentration in samples. Milli-Q water served as the blank for all sulfide measuring. It should be noted that samples containing either nickel or copper were not analyzed for sulfide due to interference from additional heavy metal in solution. Furthermore, samples containing heavy metals experienced metal-sulfide precipitation, and thus, total sulfide produced could not be determined using the Cord-Ruwisch method.

-Sulfate Measurements

Sulfate was measured using ion chromatography (IC) (Metrohm). A 10 mM standard stock solution of sodium sulfate was made and diluted in Milli-Q water to create standard solutions. The standard solutions had concentrations of 1.0, 0.8, 0.6, 0.4, 0.2, and 0.002 mM. These standard solutions were created fresh before every IC run. Eluent was comprised of 1.0 mM $NaHCO_3$ and 3.2 mM Na_2CO_3 with a flow rate of 0.7 mL/min. Regenerant used was comprised of 0.5 mM H_2SO_4 and injected with an 800 Dosino. (Metrohm). Injection volume for samples was 20 µL. Samples run were diluted either 1:50 or 1:100, depending on the possible amount of sulfate in each sample.

-Lactate/Acetate Measurements

Lactate and acetate were monitored using a Shimadzu HPLC equipped with a Bio-Rad HP-Aminex column, using 0.2 µm filtered 7.5 mM H_2SO_4 as the mobile phase (Shimadzu Scientific Equipment). Samples were injected in volumes of 50 µL. The mobile phase was set at a constant flow of 0.8 mL/min, and the column oven was set to 46 degrees C. Organic acids were analyzed with a Shimadzu SPD-10A UV-VIS detector set at 210 nm (Shimadzu Scientific Equipment).

-Real-time polymerase chain reaction (qPCR)

Quantification of gene number for the dsrA gene was monitored using a Bio Rad CFX Connect Real-Time System. Table 13 below depicts the forward and reverse primers used.

Table 13: Forward and reverse primers used.

Name	Sequence (5'-3')	Deg[a]	Target gene	Position[b]	PCR product size [bp]	Reference
DSR1F +	ACSCACTGGAA GCACGGCGG	2	*dsrA*	187-206	221	(Kondo, Nedwell, Purdy, & Silva, 2004)
DSR-R	GTGGMRCCGT GCAKRTTGG	16	*dsrA*	389-407		(Kondo et al., 2004)

[a]Degeneracy is given as the number of oligonucleotides that comprise the primer.
[b]Position is relative to *Desulfovibrio vulgaris* Hildenborough *dsrAB* gene.

The sequence for the gBlocks used to make the standard curves for *dsrAB* gene quantification can be seen below.

Sequence (5'-3')

CTGGCCCAGCTTCGTGTCCGACATCAAGCAGGAGGCTGCGTACCGGGCGGCCAACCCGA
AGGGGCTGGACTACCAGGTACCCGTCGACTGTCCGGAAGACCTGCTCGGCGTTCTCGAG
CTGTCCTACGATGAGGGTGAAACCCACTGGAAGCACGGCGGCATCGTCGGCGTGTTCGG
TTACGGCGGCGGCGTCATCGGCCGTTACTGTGACCAGCCCGAAAAGTTCCCCGGCGTGG
CGCACTTCCATACCGTGCGCGTGGCCCAGCCTTCCGGCAAGTACTACTCTGCCGACTAC
CTGCGCCAGCTGTGCGACATCTGGGACCTGCGCGGTTCCGGTCTGACCAACATGCACGG
CTCCACGGGTGACATCGTTCTCCTCGGCACGCAGACCCCCCAGCTCGAAGAAATCTTCT
TCGAACTGACCCACAACCTGAACACCGACCTTGGTGGTTCCGGTTCGAACCTGCGTACC
CCTGAATCGTGCCTCGGCAAGTCGCGTT

The gBlock sequence is adapted from the *dsrAB* gene of *Desulfovibrio vulgaris* Hildenborough, with a size of 500 base pairs and a position of 48-547 relative to the *Desulfovibrio vulgaris* Hildenborough *dsrAB* gene. Table 14 below depicts the qPCR reaction setup used, while Figure 2 depicts the thermocycler protocol.

Table 14: qPCR reaction setup.

Component	Volume per 20 µl Reaction	Final Concentration
iTaq™ Universal SYBR® Green Supermix (2x)	10 µl	1x
DSR1F+ (10 µM)	0.6 µl	300 nM
DSR-R (10 µM)	0.6 µl	300 nM
DNA template	1 µl	
Bovine Serum Albumin (10 µg/µl)	1 µl	0.5 µg/µl
H_2O	6 µl	-
Total reaction mix volume	20 µl	-

iTaq™ Universal SYBR® Green Supermix (Bio-Rad, Catalog#: 172-5121)
Bovine Serum Albumin (Roche, Catalog#: 10711454001)

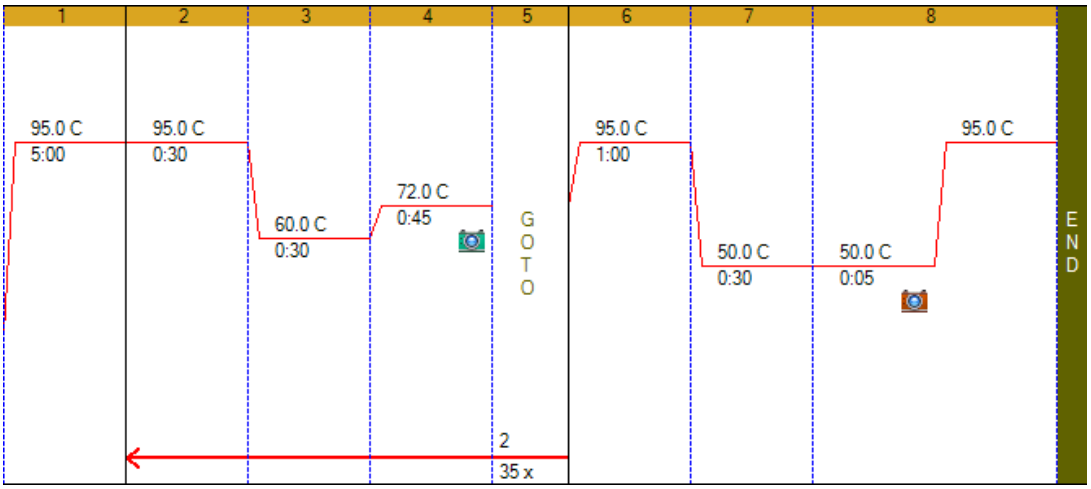

Figure 2: qPCR thermocycler protocol.

-Metal Analysis

The same metal analysis as was described above in the sorption study was also used for the metal inhibition growth studies.

-Sampling

All sampling was performed sterilely and anoxically using a Bunsen burner and gassing station containing ultra-high purity nitrogen gas. Sampling was performed with either a 5, 3, or 1 mL sterile syringe (BD Syringe) and a 25G sterile needle (BD PrecisionGlide Needle). When a sample was to be taken for metal analysis, a 5 mL syringe was used. When a sample for qPCR, sulfate/lactate/acetate, and sulfide was to be taken, a 3 mL syringe was used. When a sample for only sulfide was to be taken, a 1 mL syringe was used. Briefly, to take a sample, the syringe and needle were first degassed using UHP nitrogen. The blue butyl stopper of the serum bottle to be sampled from was flamed using 200 proof reagent alcohol. A sample could then be withdrawn from the serum bottle using the sterile and degassed syringe and needle. The same volume of nitrogen was put into the

serum bottle as liquid sample being taken out to ensure consistent pressure. All work was performed next to a Bunsen burner to ensure sterile conditions.

Next, if necessary, 1 mL of liquid sample was put into a sterile RNase/DNase free 1.5 mL centrifuge tube (USA Scientific) for qPCR analysis. The needle was then taken off the syringe and a 0.2 µm PTFE syringe filter (Millipore Millex-FG) was put on. If metal analysis was to be performed, roughly 2 mL of solution was then filtered into a 15 mL falcon tube (Corning CentriStar), and the remanence filtered into a 1.5 mL centrifuge tube (USA Scientific). If no metal analysis was needed, roughly 1.4 mL of liquid was filtered into a 1.5 mL centrifuge tube. The filtered sample contained in the 1.5 mL centrifuge tube was then used for sulfide, sulfate, and lactate/acetate analysis. 0.25 mL of the filtered sample was used to perform the sulfide analysis method as described earlier. 1 mL of the remaining solution was then pipetted into a 15 mL falcon tube containing 9 mL of Milli-Q water so as to dilute the sample 1:10 for sulfate and/or lactate and acetate analysis. These sulfate/lactate/acetate samples were degassed for 5 min by vigorous bubbling of UHP nitrogen into the sample before storage. This was done to ensure no sulfide was left in the samples. All samples were stored at -20 degrees C. Roughly, 5 mL of sample was needed for all analyses to be performed, 3 mL for all analyses minus metal analysis, and 1 mL for only sulfide analysis.

-*Statistics*

Single factor Analysis of variance (ANOVA) statistics tests were performed in Excel. (Microsoft). Furthermore, paired t-tests were also performed in Excel as needed following ANOVA results. These tests were used to determine if any statistically

significant differences in growth rates or total cell yield existed in the batch growth and copper inhibition growth experiments. Total cell yield was defined to be the maximum number of cells obtained during a growth experiment.

Results

-Metal Sorption onto Tested Biochars

Overall, both $MgCl_2$ and $MgOH_2$ modified biochars were found to significantly increase copper sorption as compared to the unmodified biochar. The copper sorption isotherms for the tested biochars can be seen in Figure 3 and Figure 4 below. The peculiar upward trending $MgCl_2$ biochar copper sorption isotherm should be noted. It was noticed during testing that the $MgCl_2$ copper itself had residual copper on it, which can also be seen in Table 1. This is most likely due to residual copper left on the biochar during the process of producing/pyrolyzing this modified biochar. This residual copper was released from the biochar during the sorption process, masking the true sorption capacity of the biochar at decreasing copper concentrations, and thus, leading to the upward trending fit line.

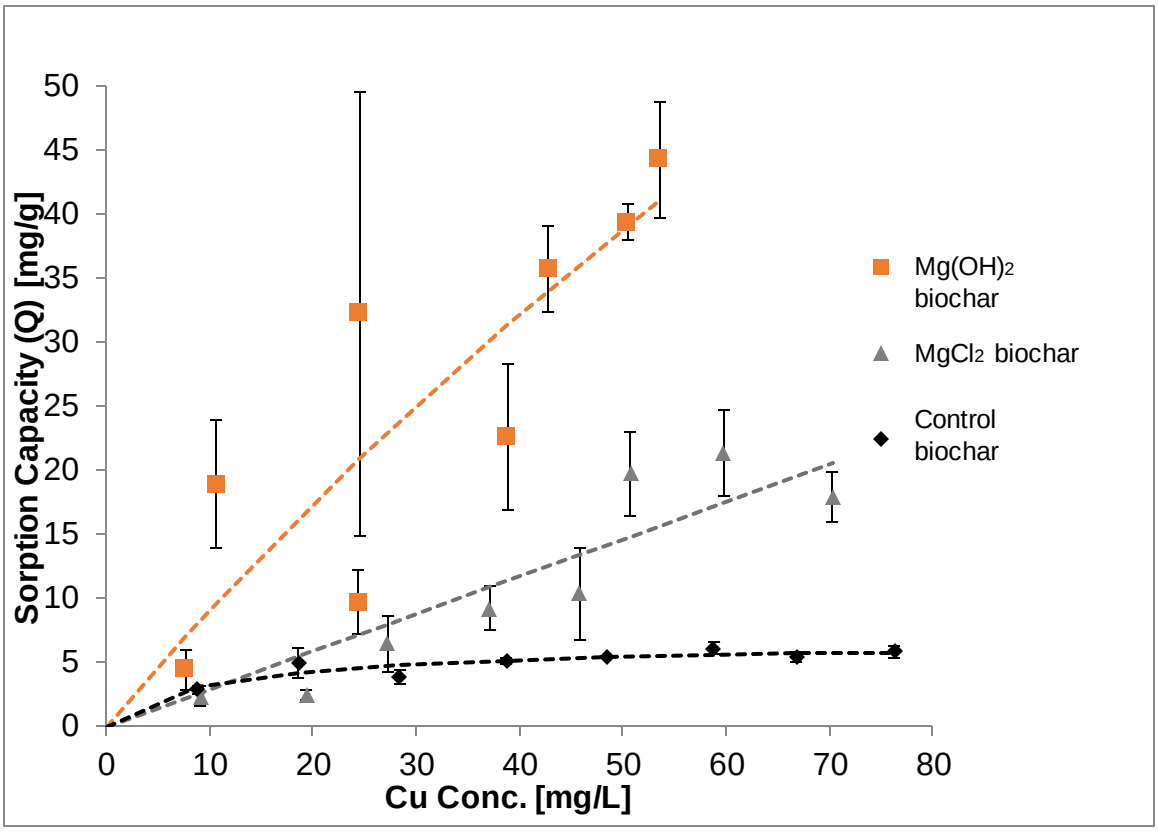

Figure 3: Sorption isotherms for copper onto tested biochars. Fitted lines represent best fit lines based on Langmuir fitting. The standard deviation between the triplicate samples is shown in the error bars.

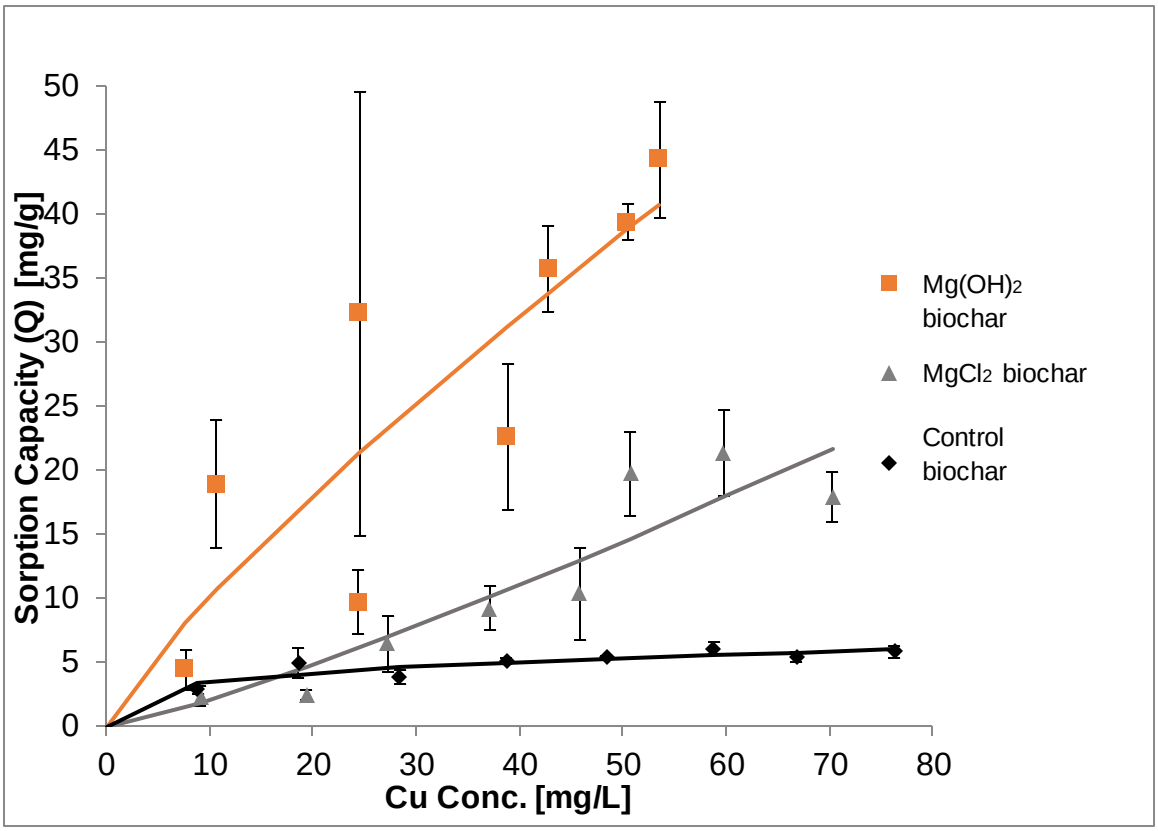

Figure 4: Sorption isotherms for copper onto tested biochars. Fitted lines represent best fit lines based on Freundlich fitting. The standard deviation between the triplicate samples is shown in the error bars.

Table 15 below shows the results of fitting both the Langmuir and Freundlich models to the isotherms. Overall, based on Langmuir fitting, the unmodified and $MgOH_2$ modified biochars were found to have sorption capacities of 6.6 and 210 mg/L, respectively. This is roughly a 30-fold increase in copper sorption capacity for the $MgOH_2$ modified biochar as compared to the unmodified biochar. The $MgCl_2$ Langmuir results were not able to be fit due to the upward trending isotherm of the $MgCl_2$ biochar. Both the Langmuir and the Freundlich fitting resulted in very similar R^2 values for all biochars.

Table 15: Copper isotherm fitting results using Langmuir and Freundlich models.

Copper Sortion (pH = 4.0)		
Langmuir	**Q max [mg/g]**	**R^2 Value**
Swiss	6.56	0.77
$MgCl_2$	N.A.	N.A.
$Mg(OH)_2$	213	0.70
Freundlich		
Swiss	---	0.76
$MgCl_2$	---	0.84
$Mg(OH)_2$	---	0.70

Nickel sorption isotherms for the tested biochars can be seen in Figure 5 and Figure *6* below. As observed with the copper sorption isotherms, the modified biochars sorbed more nickel than the unmodified biochar, with $MgOH_2$ possessing the greatest sorption capacity. The $MgOH_2$ sorption isotherm, like the $MgCl_2$ copper sorption isotherm, could not be fitted using the Langmuir model. This is due to the upward trend in the sorption data. This is most likely due to the high degree of uncertainty between triplicate samples.

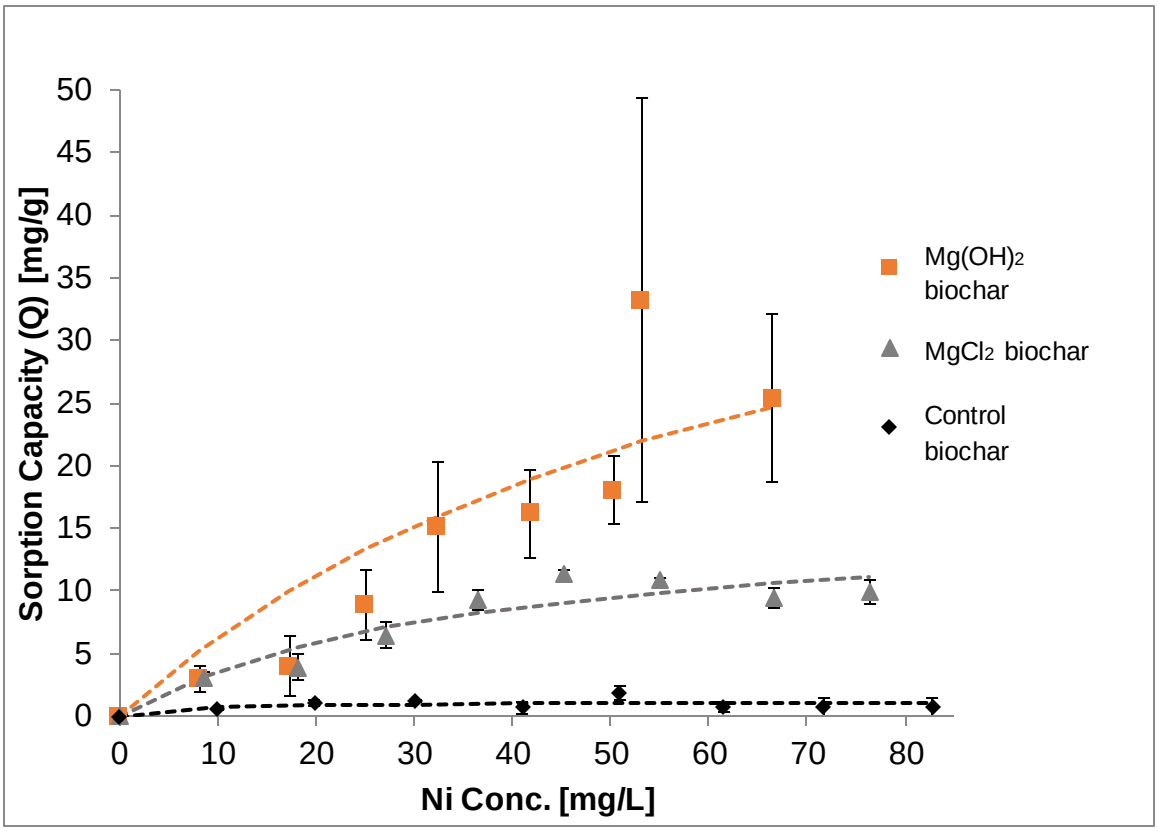

Figure 5: Sorption isotherms for nickel onto tested biochars. Fitted lines represent best fit lines based on Langmuir fitting. The standard deviation between the triplicate samples is shown in the error bars.

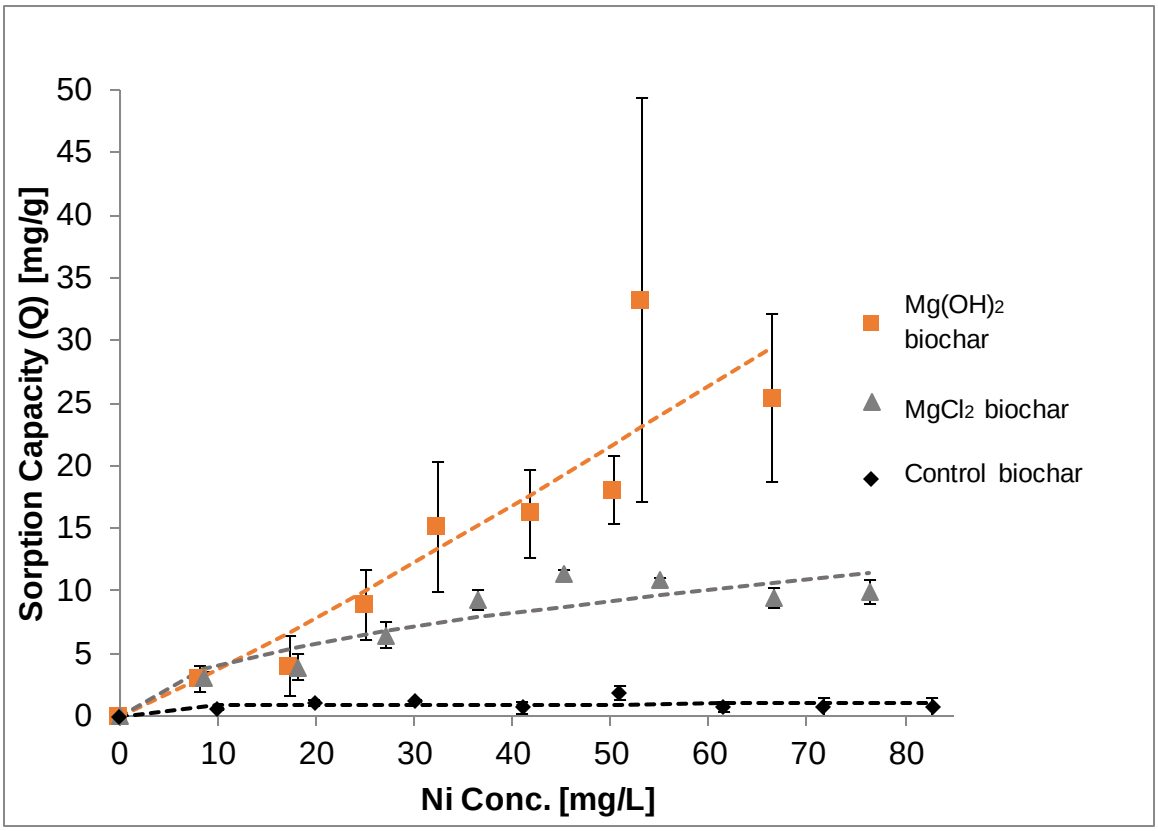

Figure 6: Sorption isotherms for nickel onto tested biochars. Fitted lines represent best fit lines based on Freundlich fitting. The standard deviation between the triplicate samples is shown in the error bars.

Table 16 below shows the results of fitting the nickel sorption isotherms to both the Langmuir and Freundlich models. Overall, the $MgCl_2$ modified biochar had a nickel sorption capacity of 16.1 mg/g, a 16-fold increase in sorption capacity as compared to the unmodified biochar. The $MgOH_2$ biochar could not be fitted to the Langmuir model, but visual inspection of Figure 5 clearly shows it had the greatest nickel sorption capacity.

Table 16: Nickel isotherm fitting results using Langmuir and Freundlich models.

Nickel Sorption (pH = 4.0)		
Langmuir	**Q max [mg/g]**	**R^2 Value**
Swiss	1.05	0.038
$MgCl_2$	16.1	0.82
$Mg(OH)_2$	N.A.	N.A.
Freundlich		
Swiss	---	0.006
$MgCl_2$	---	0.75
$Mg(OH)_2$	---	0.80

-D. alaskensis Growth in Presence of Biochar

The sulfate concentrations at different times during the *D. alaskensis* growth curve experiment in the presence of varying doses of biochar can be seen in Figure 7 below. Visual examination of Figure 7 shows that biochar had no effect on sulfate reduction rates during *D. alaskensis* growth.

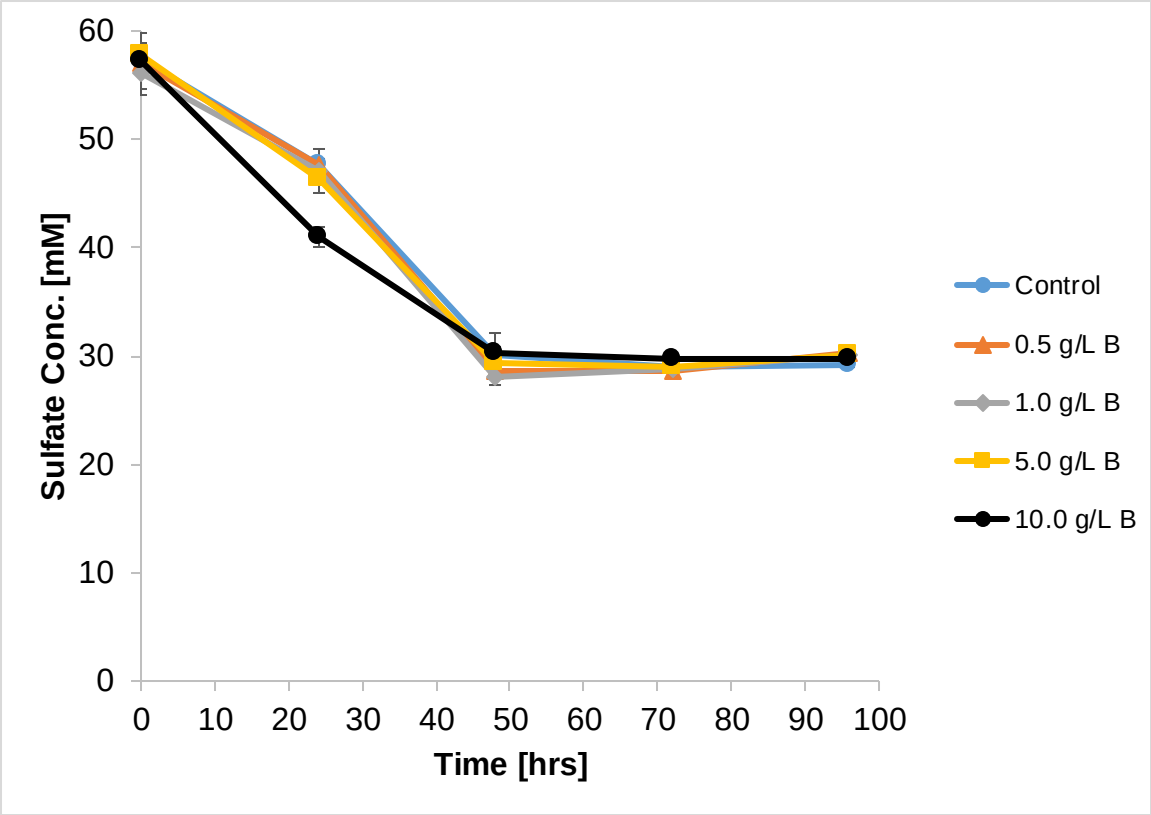

Figure 7: Sulfate concentration versus time for the *D. alaskensis* growth curve experiment in the presence of varying doses of biochar. The control series did not contain any biochar. 0.5 g/L B series represent the biotic data for the samples containing a dose of 0.5 g/L of biochar. All other series are labeled likewise. Error bars represent the standard deviation between triplicate samples.

Furthermore, sulfide concentration versus time is shown in Figure 8 below. When comparing Figure 7 to Figure 8, it can be seen that all sulfate that is reduced is completely reduced to sulfide. This is as expected since *D. alaskensis* is a complete sulfate reducer (capable of completely reducing sulfate to sulfide).

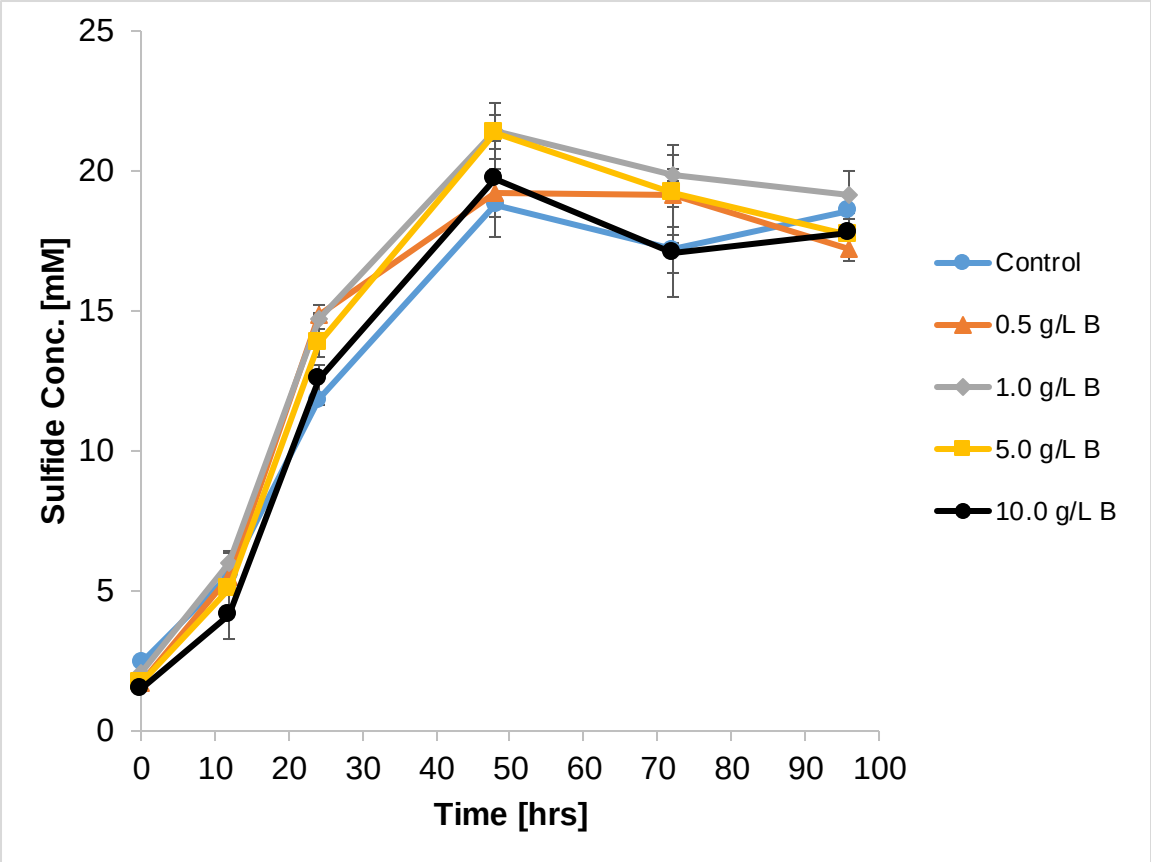

Figure 8: Sulfide concentration versus time for the *D. alaskensis* growth curve experiment in the presence of varying doses of biochar. Error bars represent the standard deviation between triplicate samples.

The complete qPCR results depicting *D. alaskensis* cells per milliliter combined with the sulfate concentration data can be seen in Figure 9 below. From this figure, it can be seen that the observed sulfate reduction corresponded with cell growth.

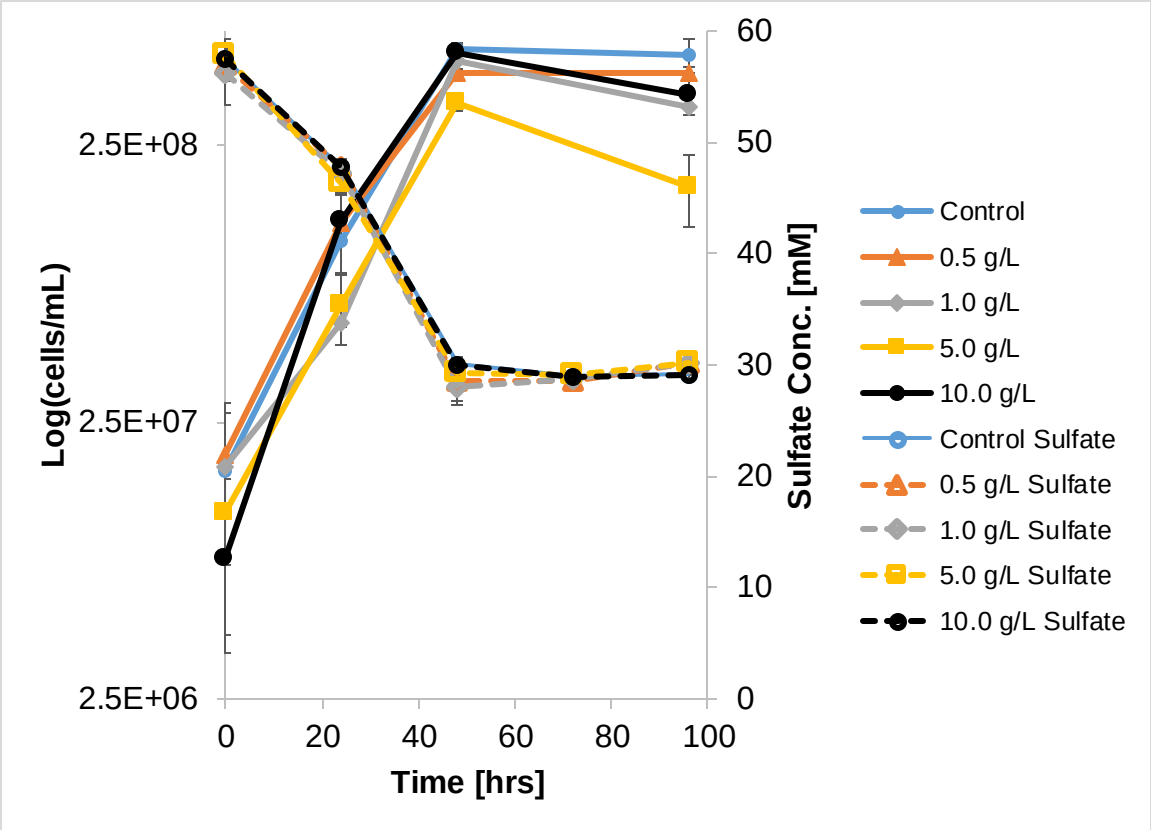

Figure 9: Complete qPCR data for *D. alaskensis* growth in the presence of biochar combined with sulfate concentration data. Control series contained no biochar. 0.5 g/L represents a dose of 0.5 g/L of biochar. Error bars represent the standard deviation between triplicate samples.

Table 17 below shows the complete results for the SGR, including averages and standard deviations These plots can be seen in Appendix C: *D. alaskensis* Log Growth Figures. Statistical analysis of this data results in no significant differences in SGR between series [p-value of 0.56]. This is in agreement with the sulfate consumption and sulfide production graphs (Figure 7 and Figure 8). Statistical analysis of the total cell yield, however, leads to an ANOVA p-value of 0.00068. This means that the total cell yield was not the same between treatments. Table 18 below shows the results of the paired t-tests comparing each

treatment to the control. As can be seen in this table, the 0.5 and 5.0 g/L treatments resulted in a lower cell yield than the control.

Table 17: Specific growth rate (SGR [1/hr]) results for each series and individual samples within a series.

Triplicate Sample	SGR for Triplicate Sample				
	1 (0.5 g/L)	2 (1.0 g/L)	3 (5.0 g/L)	4 (10.0 g/L)	5 (Control)
SGR-1	0.0633	0.0592	0.0822	0.0836	0.0668
SGR-2	0.0608	0.0896	0.0702	0.1025	0.0652
SGR-3	0.0795	0.0737	0.0647	0.0831	0.1207
Average SGR	**0.0679**	**0.0742**	**0.0724**	**0.0897**	**0.0842**
Standard Deviation	0.0102	0.0152	0.0089	0.0111	0.0316

Table 18: Total cell yield paired t-test results.

Triplicate Sample	Total Cell Yield [cells/mL]				
	1 (0.5 g/L)	2 (1.0 g/L)	3 (5.0 g/L)	4 (10.0 g/L)	5 (Control)
SGR-1	4.75E+08	5.51E+08	3.80E+08	5.93E+08	5.55E+08
SGR-2	4.48E+08	5.44E+08	3.67E+08	5.23E+08	5.85E+08
SGR-3	4.51E+08	4.24E+08	3.30E+08	5.17E+08	5.54E+08
Average	**4.58E+08**	**5.06E+08**	**3.59E+08**	**5.44E+08**	**5.65E+08**
Standard Deviation	1.48E+07	7.17E+07	2.59E+07	4.20E+07	1.77E+07
Paired T-Test P-Value (Compared to Control)	0.023	0.26	0.0055	0.57	---

Figure 10 and Figure 11 below depict lactate consumption and acetate production, respectively, throughout the course of the whole experiment. These figures show a one to one relationship between lactate consumption to acetate production, as would be expected based on D. alaskensis metabolism. No difference between each series for either the lactate or acetate graph can be noticed. This agrees with the specific growth rate data in which no differences can be perceived. Furthermore, from the sulfate data in Figure 7, it can be seen that about 30 mM of sulfate is reduced to sulfide during the course of the experiment. To

reduce one molecule of sulfate to sulfide, 8 electrons are needed. The oxidation of one molecule of lactate to acetate releases 4 electrons. Thus, 2 moles of lactate are needed to reduce one mole of sulfate to sulfide. With 30 mM of sulfate being reduced to sulfide throughout the course of the experiment, 60 mM of lactate being consumed throughout agrees stoichiometrically with the sulfate results.

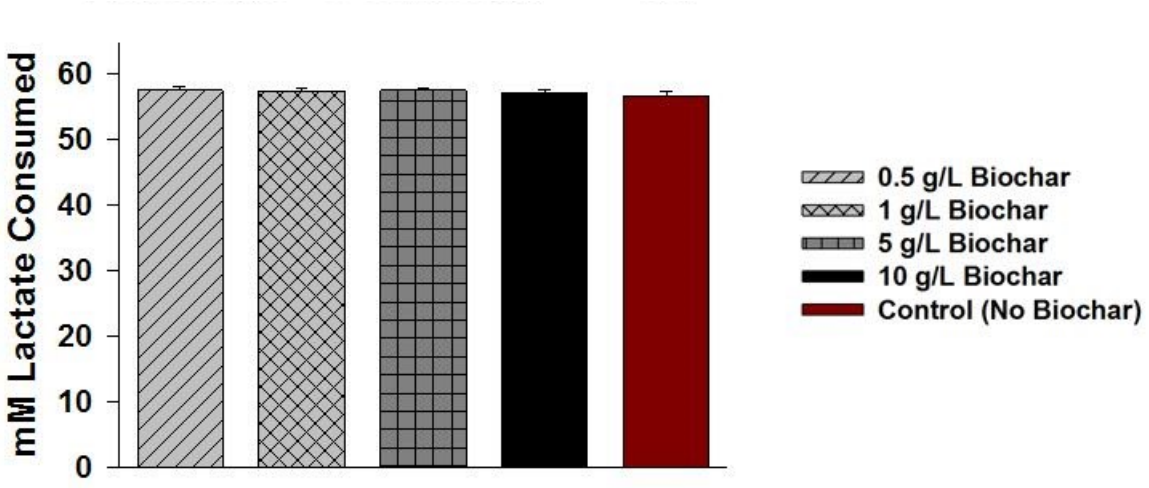

Figure 10: Lactate consumption for each series during the course of the whole experiment. Error bars represent standard deviation between triplicate samples within a series.

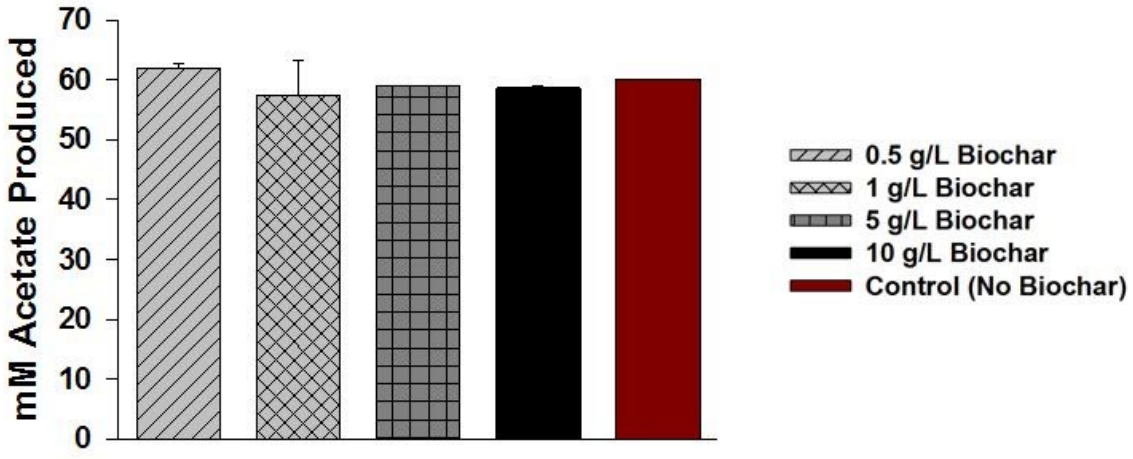

Figure 11: Acetate production for each series during the course of the whole experiment. Error bars represent standard deviation between triplicate samples within a series.

-D. alaskensis Metal Inhibition Growth

The sulfate concentrations at different times during the *D. alaskensis* growth experiment in the presence of varying copper concentrations and 1.0 g/L biochar can be seen in Figure 12-14. Not all copper growth series were plotted on the same graph. This was done for ease of examination. Furthermore, the 1.0 mg/L copper experiment is plotted on its own graph. This is due to the fact that the 1.0 mg/L copper test was performed after the initial copper tests, and thus, a new control series had to be included. As can be seen in the below mentioned figures, copper concentrations over 2.5 mg/L resulted in the complete inhibition of sulfate reduction over the course of the experiment, regardless of if biochar was present. However, by visual inspection of Figure 12, the addition of 1.0 g/L of biochar appeared to reduce copper inhibition at 0.5 mg/L. Figure 14, however, depicts that once the copper concentration reached 1.0 mg/L, the addition of 1.0 g/L of biochar did not mitigate copper inhibition.

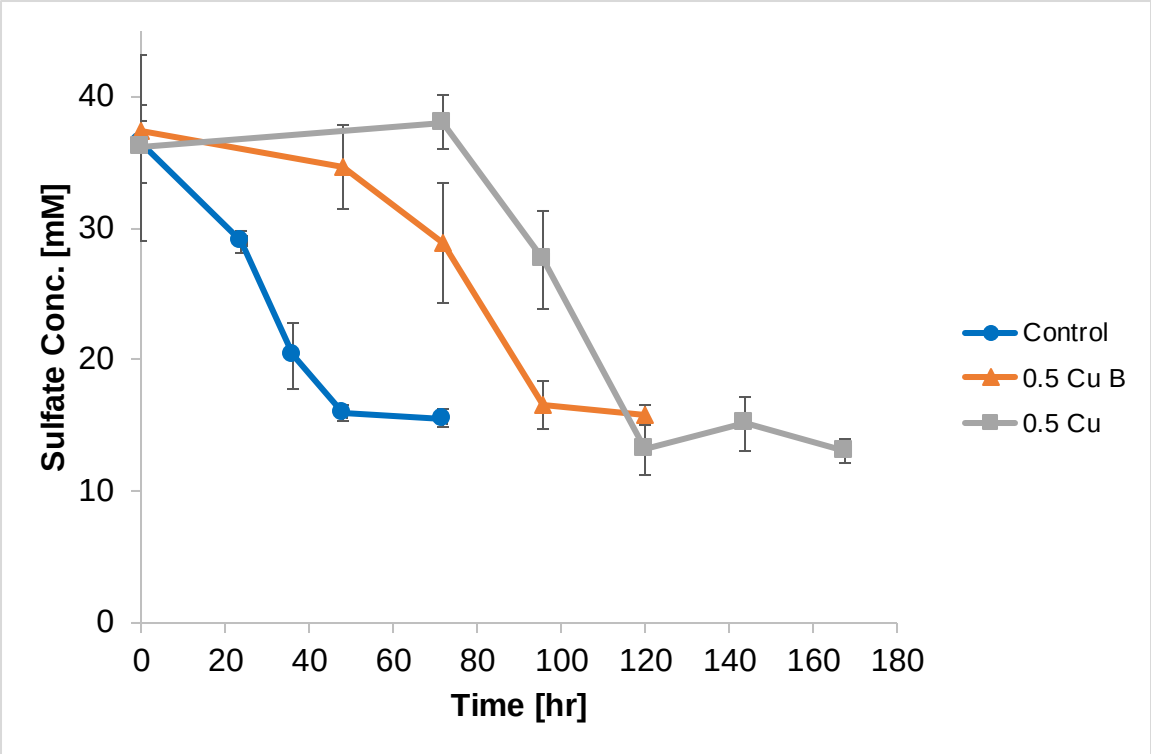

Figure 12: Sulfate concentration versus time for the copper inhibition *D. alaskensis* growth experiment in the presence of 1.0 g/L biochar and 0.5 mg/L copper. 0.5 Cu represents 0.5 mg/L copper concentration. Series that contained biochar are represented with a B. Error bars represent the standard deviation between triplicate samples.

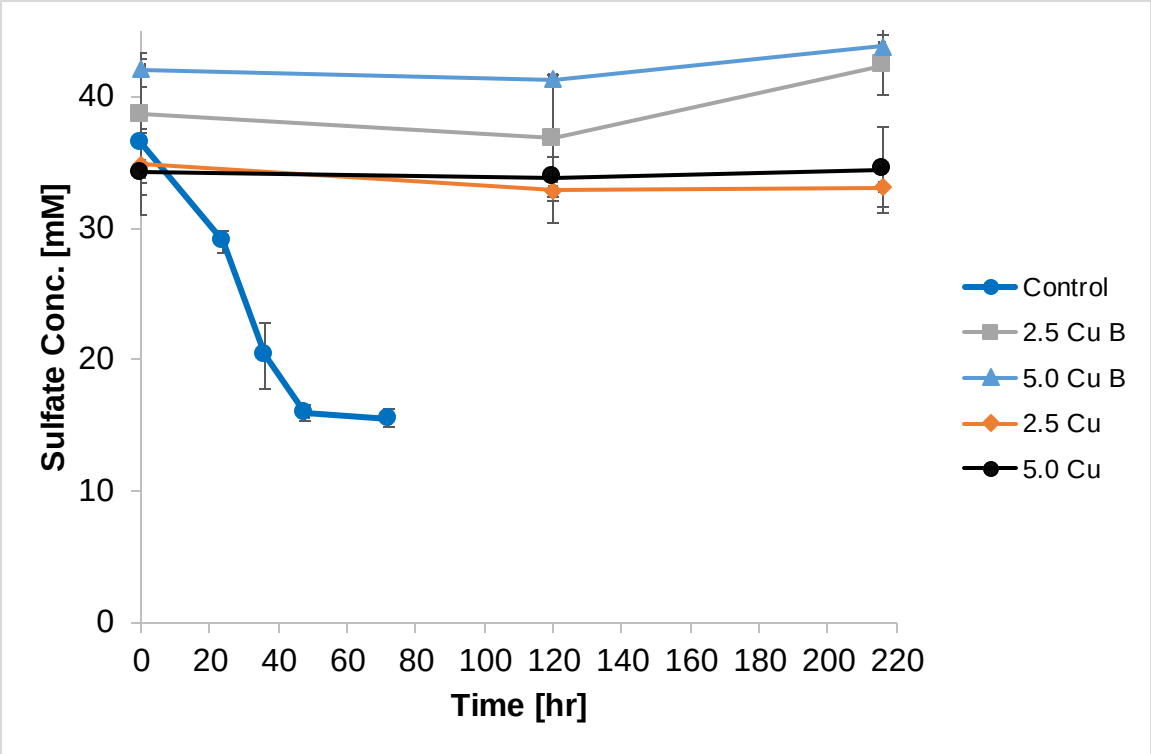

Figure 13: Sulfate concentration versus time for the copper inhibition *D. alaskensis* growth experiment in the presence of 1.0 g/L biochar. 2.5 Cu represents 2.5 mg/L copper concentration. Series that contained biochar are represented with a B. Error bars represent the standard deviation between triplicate samples.

The 1.0 mg/L copper growth experiment data does not present a clear trend like the 0.5 mg/L copper growth curve did (see Figure 14). This was due to the fact that all triplicates in the 1.0 mg/L copper experiment series did not initiate growth after the same lag time. Thus, sulfate error bars are large and the sulfate reduction curves do not show a clean decrease. An abiotic control composed of 1.0 g/L biochar, 2.5 mg/L copper, and no cells was also included. No sulfate reduction was seen in this abiotic control (Figure 35 in Appendix D: Abiotic Copper Metal Inhibition Control).

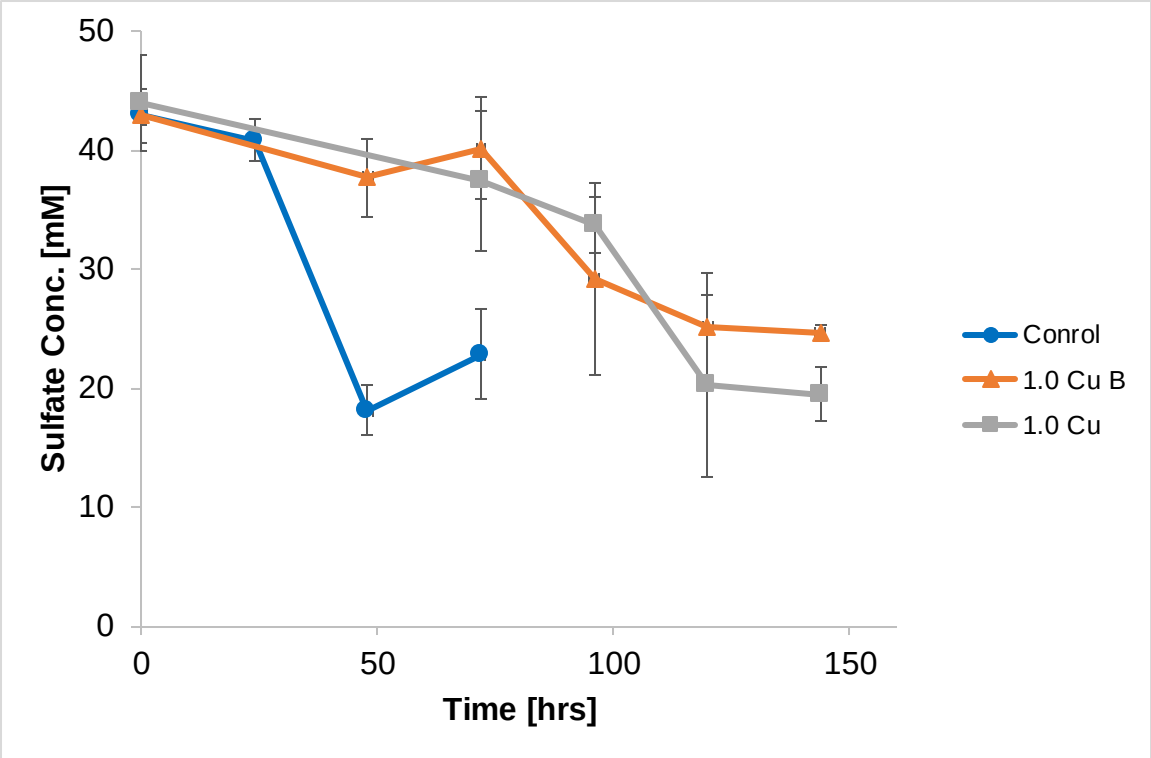

Figure 14: Sulfate concentration versus time for the 1.0 mg/L copper inhibition experiment with *D. alaskensis*. 1.0 Cu represents 1.0 mg/L copper concentration. Series that contained biochar are represented with a B. Error bars represent the standard deviation between triplicate samples.

The complete qPCR results depicting *D. alaskensis* cells per milliliter combined with the sulfate concentration data can be seen in Figure 15 and Figure 16 below. From these figures, it can be seen that sulfate reduction corresponds with cell growth.

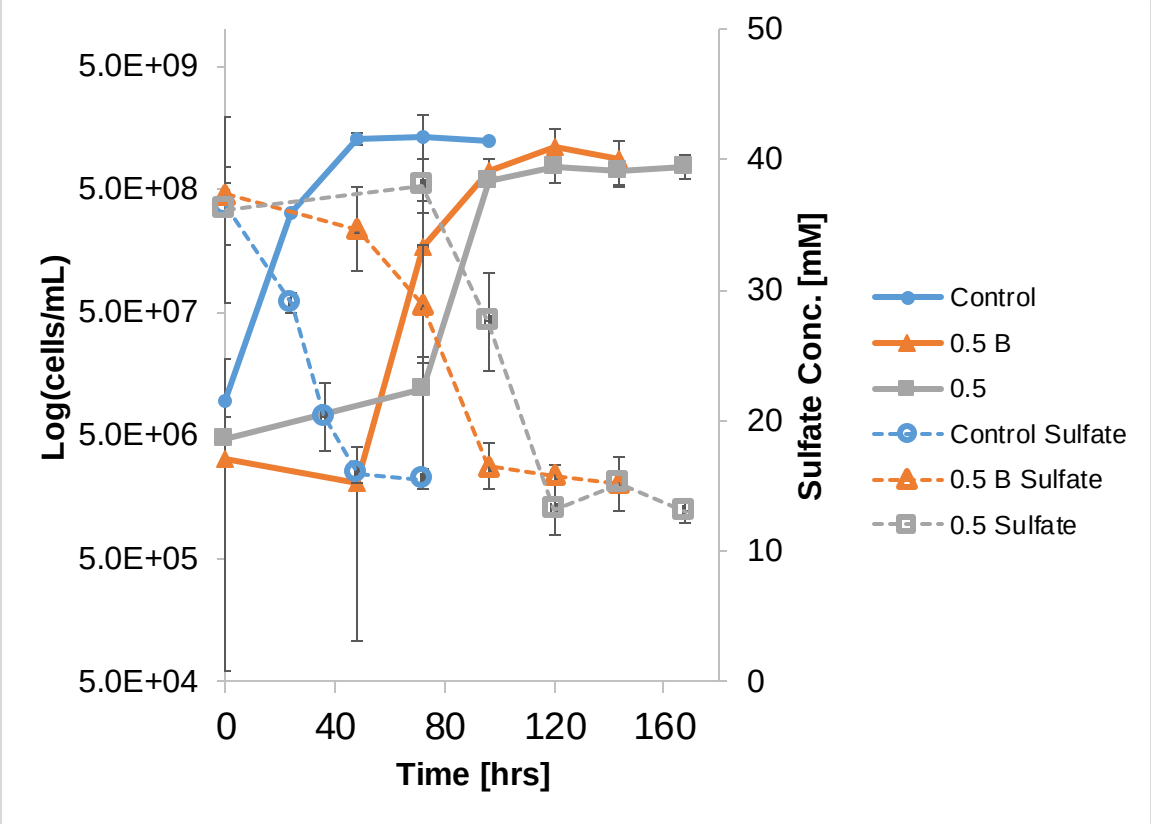

Figure 15: Complete 0.5 mg/L copper inhibited qPCR data for *D. alaskensis* growth combined with sulfate concentration data. 0.5 Cu represents 0.5 mg/L copper concentration. Series that contained biochar are represented with a B. Error bars represent the standard deviation between triplicate samples.

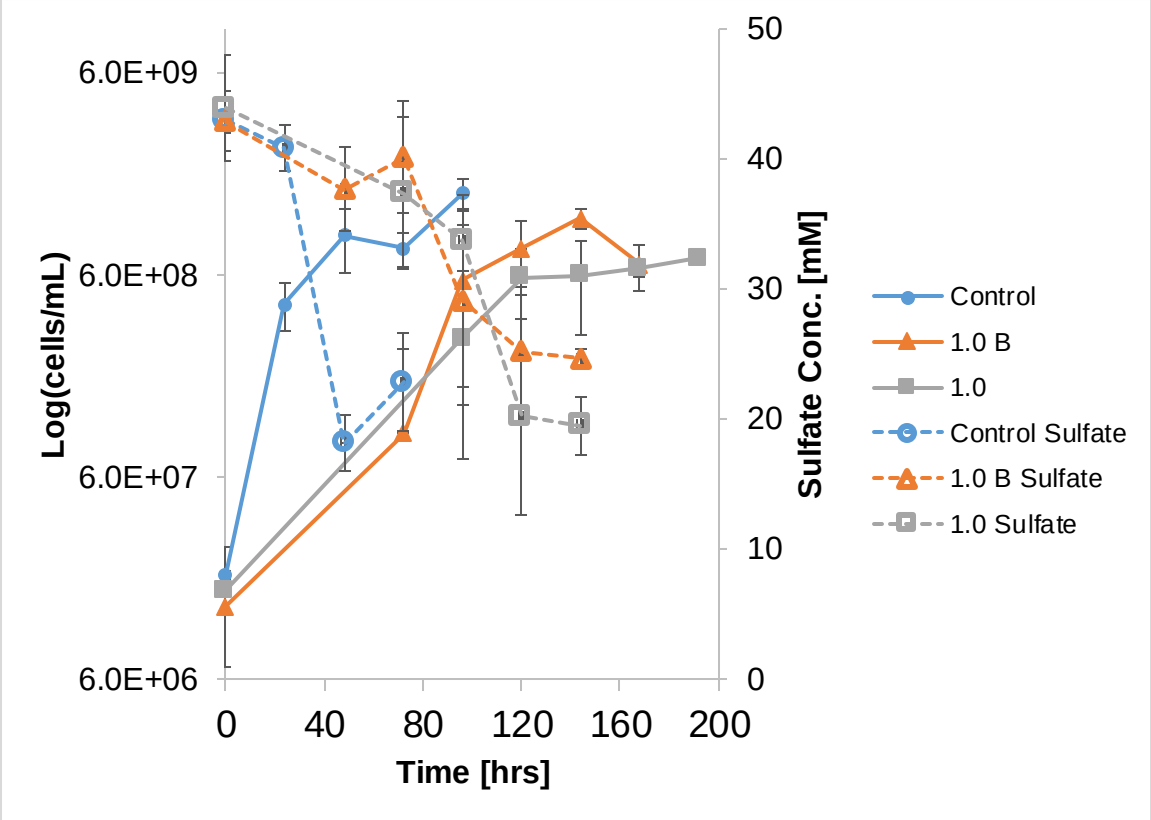

Figure 16: Complete 1.0 mg/L copper inhibited qPCR data for D. alaskensis growth combined with sulfate concentration data. 1.0 Cu represents 1.0 mg/L copper concentration. Series that contained biochar are represented with a B. Error bars represent the standard deviation between triplicate samples.

Table 19 and Table *20* below shows the complete results for the specific growth rate (SGR) from each treatment. SGR was determined by plotting the log of the cell number during exponential growth to obtain a linear line. These plots can be seen in Appendix C: *D. alaskensis* Log Growth Figures. Statistical ANOVA analysis for each SGR series leads to the conclusion that there is no statistically significant difference in SGR between any of the treatments [p-values of 0.20 and 0.097 for the 0.5 and 1.0 mg/L copper experiments, respectively].

Table 19: Specific growth rate (SGR [1/hr]) results for each series and individual samples within a series. This table represents the 0.5 mg/L copper inhibition experiment.

Triplicate Sample	Specific Growth Rate (SGR)		
	Control	**0.5 Cu Biochar**	**0.5 Cu**
SGR-1	0.124	0.104	0.103
SGR-2	0.129	0.138	0.066
SGR-3	0.082	0.138	0.100
Average SGR	**0.112**	**0.127**	**0.090**
St. Deviation	0.0259	0.0195	0.0206

Table 20: Specific growth rate (SGR [1/hr]) results for each series and individual samples within a series. This table represents the 1.0 mg/L copper inhibition experiment.

Triplicate Sample	Specific Growth Rate (SGR)		
	Control	**1.0 Cu Biochar**	**1.0 Cu**
SGR-1	0.088	0.007	0.011
SGR-2	0.081	0.099	0.026
SGR-3	0.074	0.008	0.004
Average SGR	**0.081**	**0.038**	**0.014**
St. Deviation	0.0069	0.0527	0.0111

Total cell yields from each copper inhibition experiment can be seen in Table 21 andTable *22* below. The ANOVA statistical results from the 0.5 and 1.0 mg/L copper experiments resulted in p-values of 0.42 and 0.0048, respectively. Thus, only the 1.0 mg/L copper experiment showed any statistically significant difference in total cell yield. The results of the paired t-test for the 1.0 mg/L copper experiment can also be seen in Table *22*. These results show that the control and the biochar treatment resulted in a statistically insignificant difference in cell number, while the control and the treatment without biochar resulted in a statistically significant difference in cell number [p-values of 0.13 and 0.046, respectively]. Furthermore, a paired t-test between the biochar treatment and the one without biochar also resulted in statically significant results [p-

value of 0.031]. Thus, it appears that the 1.0 mg/L copper treatment without biochar lead to a lower total cell yield than the one with biochar.

Table 21: Total cell yield for 0.5 mg/L copper inhibition experiment.

Triplicate Sample	Total Cell Yield [cells/mL]		
	Control	0.5 Cu Biochar	0.5 Cu
SGR-1	6.00E+08	1.60E+09	8.73E+08
SGR-2	1.95E+09	7.14E+08	8.63E+08
SGR-3	1.39E+09	1.06E+09	5.79E+08
Average	**1.31E+09**	**1.12E+09**	**7.71E+08**
Standard Deviation	6.80.E+08	4.44.E+08	1.67.E+08

Table 22: Total cell yield and paired t-test results for 1.0 mg/L copper inhibition experiment.

Triplicate Sample	Total Cell Yield [cells/mL]		
	Control	1.0 Cu Biochar	1.0 Cu
SGR-1	1.69E+09	1.30E+09	7.27E+08
SGR-2	1.71E+09	1.07E+09	7.03E+08
SGR-3	1.21E+09	1.09E+09	7.58E+08
Average	**1.54E+09**	**1.15E+09**	**7.29E+08**
Standard Deviation	2.85E+08	1.30E+08	2.77E+07
Paired T-Test P-Value (Compared to Control)	---	0.13	0.046

Sulfate levels measured during the nickel toxicity experiment were very erratic. This is most likely due to complications due to the presence of nickel during ion chromatography. Due to the erratic sulfate measurements, nickel toxicity data is not included in this section. Instead, it can be found in Appendix F: Nickel Inhibition of *D. alaskensis* Growth Sulfate Measurements. Furthermore, a follow-up nickel inhibition study could not be conducted due to IC trouble at the Research Analytical Laboratory.

- *D. alaskensis Cell Suspension in the Presence of Biochar*

During a resting cell suspension, no growth of the cells takes place. It is purely a measure of metabolic activity of the microbes in the suspension. The sulfate concentration versus time for different doses of biochar can be seen in Figure 17 and 18 below. As can be seen in Figure 18, no sulfate/biochar interaction happened in the abiotic controls. However, in the biotic data in Figure 17, it can be seen that, regardless of the biochar dose, biochar increased sulfate reduction rates to the same extent as compared to the control with no biochar.

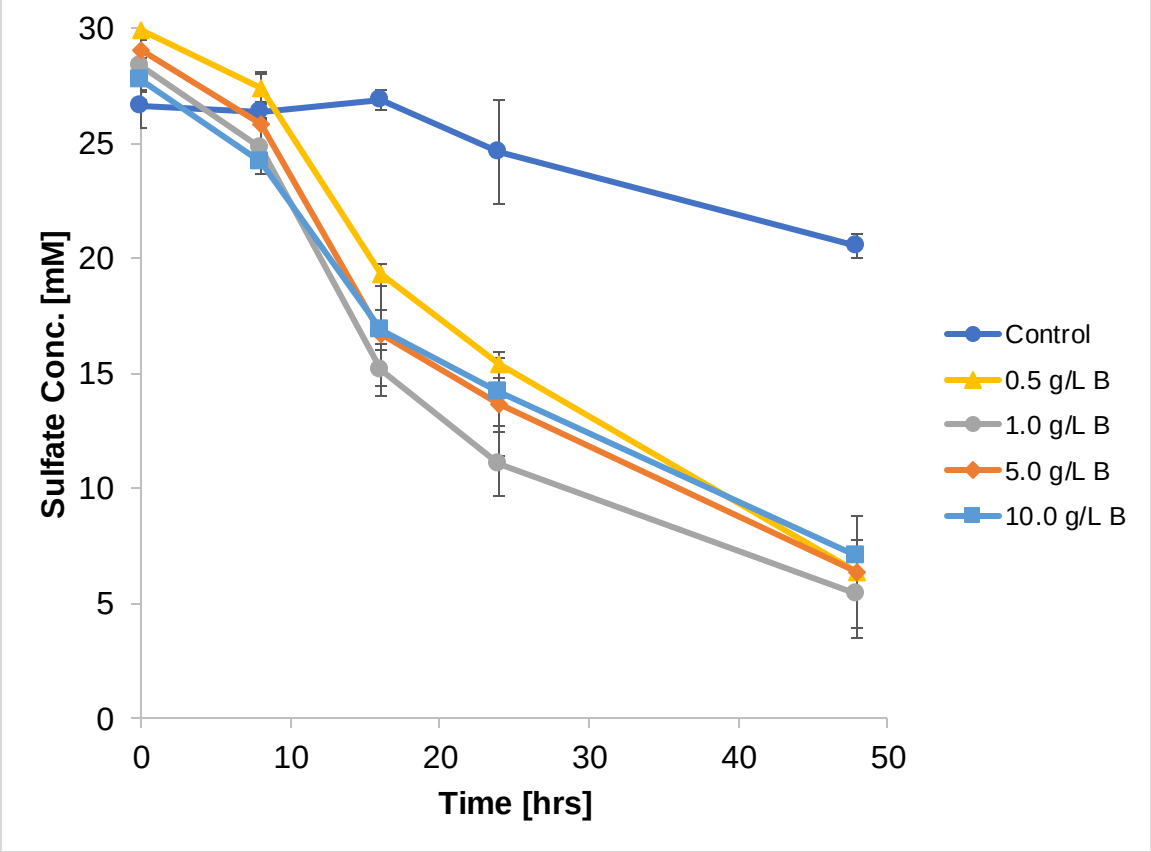

Figure 17: Sulfate concentration versus time for the *D. alaskensis* resting cell suspension experiment in the presence of varying doses of biochar. The control series did not contain any biochar. 0.5 g/L B series represent the biotic data for the samples containing a dose of 0.5 g/L of biochar. All other series are labeled likewise. Error bars represent the standard deviation between triplicate samples.

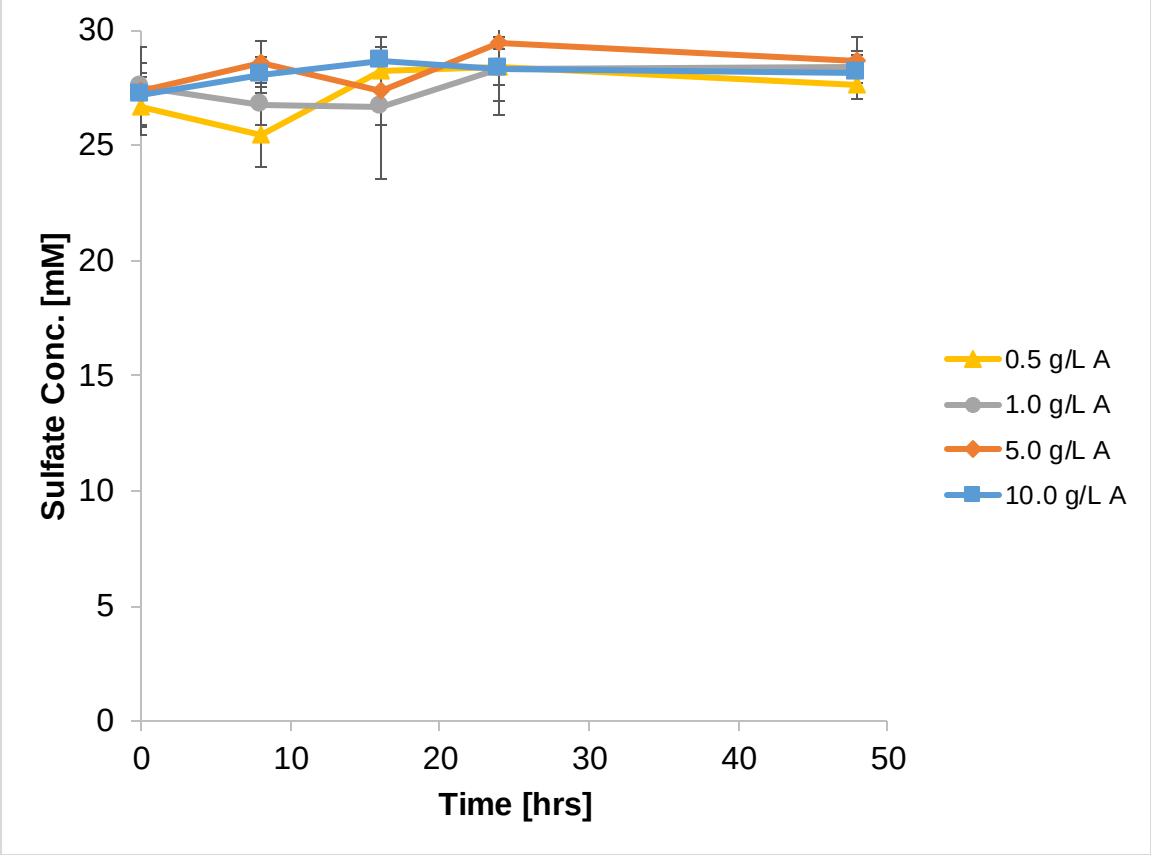

Figure 18: Sulfate concentration versus time for the *D. alaskensis* resting cell suspension experiment in the presence of varying doses of biochar. This graph shows the abiotic data (no *D. alaskensis* added). Error bars represent the standard deviation between triplicate samples.

Furthermore, the biotic and abiotic sulfide data in Figure 19 and Figure *20* agree with the above sulfate data. Both sulfate and sulfide graphs show a roughly one to one correspondence as would be expected metabolically.

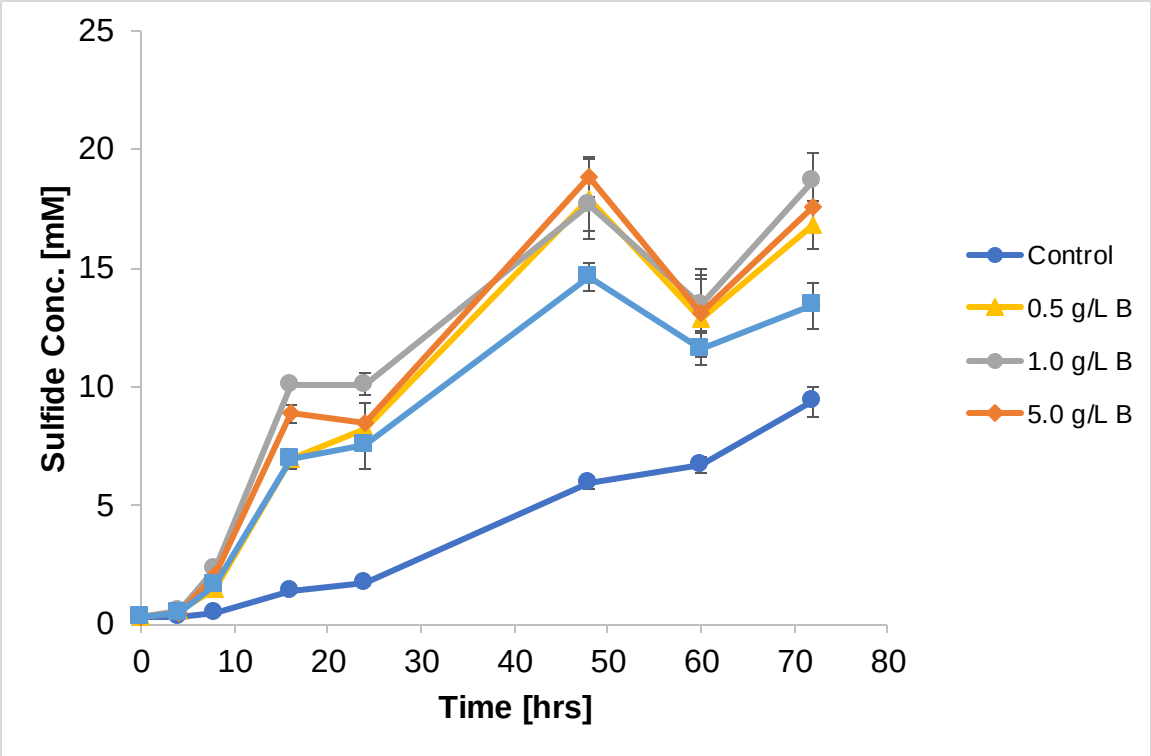

Figure 19: Sulfide concentration versus time for the *D. alaskensis* resting cell suspension experiment in the presence of varying doses of biochar. Error bars represent the standard deviation between triplicate samples.

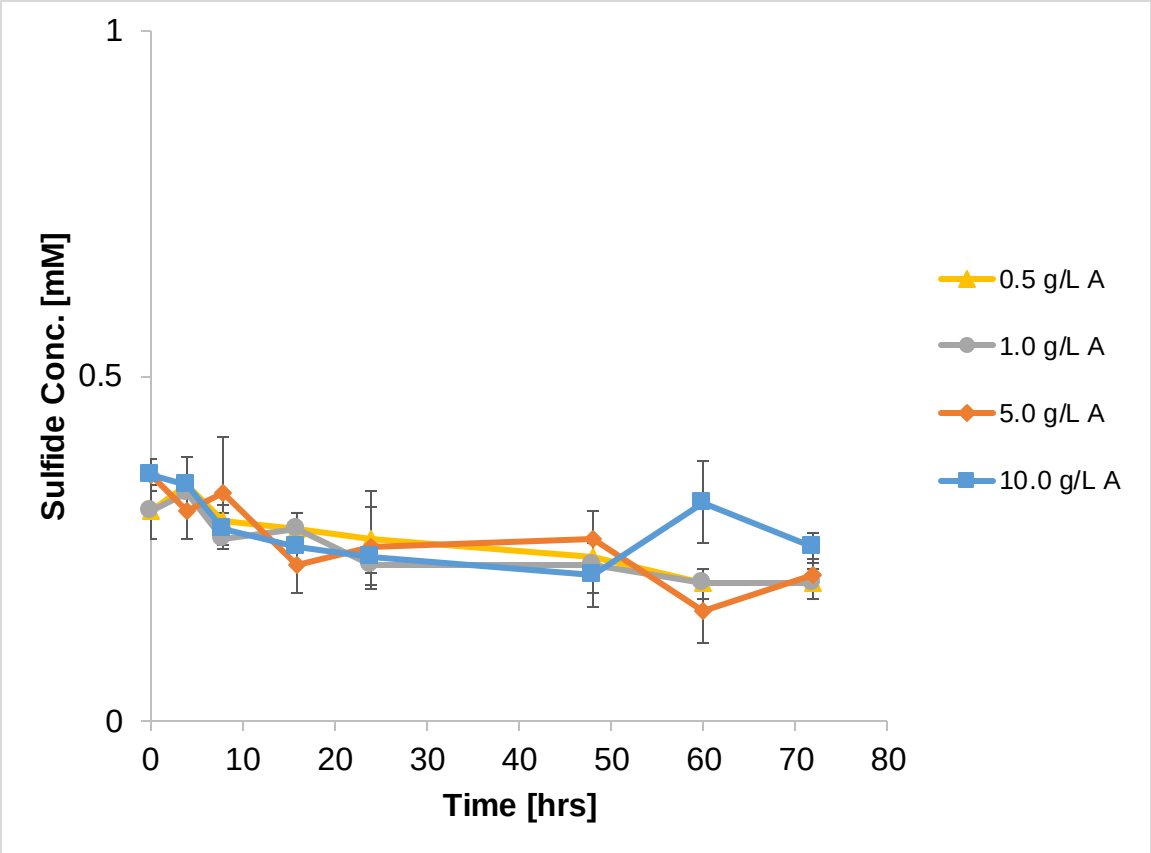

Figure 20: Sulfide concentration versus time for the *D. alaskensis* resting cell suspension experiment in the presence of varying doses of biochar. This graph shows the abiotic data (no *D. alaskensis* added). Error bars represent the standard deviation between triplicate samples.

Lactate consumption and acetate production throughout the whole experiment can be seen in Figure 21 and Figure *22*, respectively. As in the growth experiment, the oxidation of one mole of lactate by *D. alaskensis* should result in one mole of acetate. This roughly seems to be the case based on the lactate and acetate results below. Furthermore, as explained before, two moles of lactate are necessary for one mole of sulfate to be completely reduced to sulfide. This is the case when examining Figure 17, the sulfate data, and Figure 21, the lactate data.

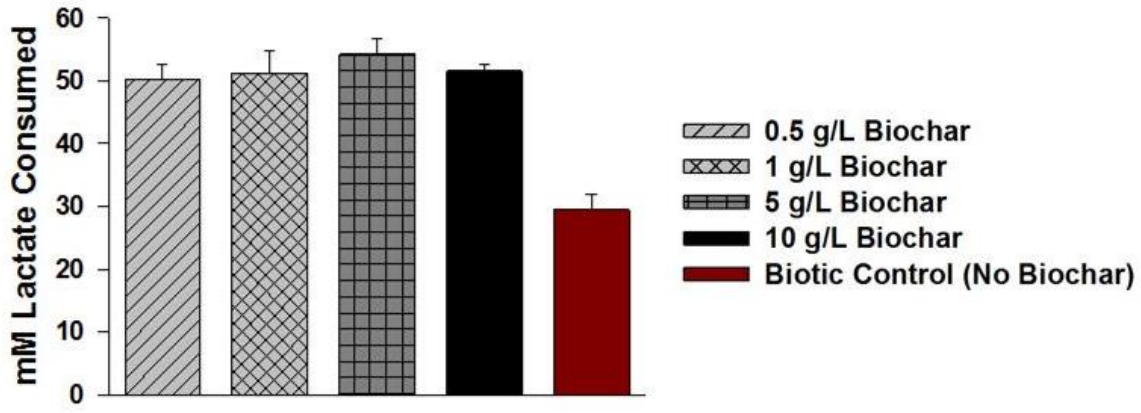

Figure 21: Lactate consumption for each series during the course of the whole experiment. Error bars represent standard deviation between triplicate samples within a series.

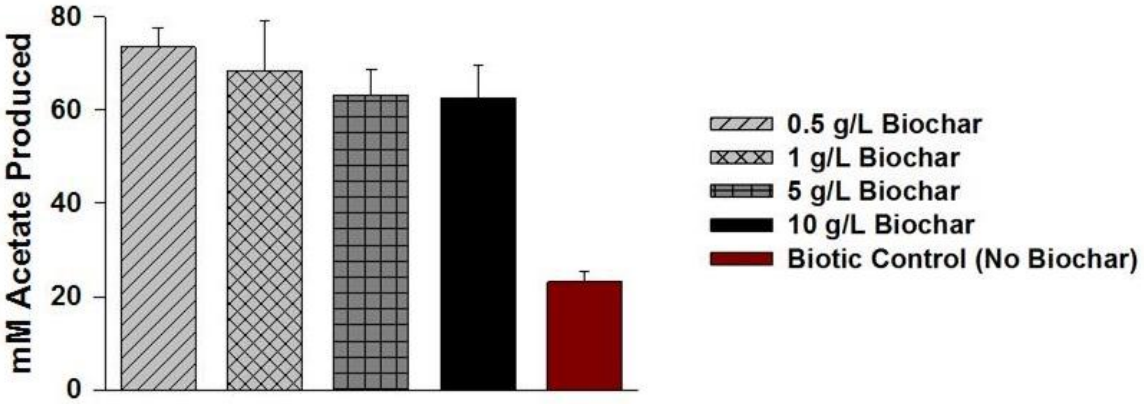

Figure 22: Acetate production for each series during the course of the whole experiment. Error bars represent standard deviation between triplicate samples within a series.

Discussion

Modified biochar, created by pre-soaking the biomass before pyrolysis in either $Mg(OH)_2$ or $MgCl_2$ solution, was found to significantly increase sorption capacities towards both copper and nickel in solution, as compared to unmodified biochar (Figure 3 and Figure 5). $Mg(OH)_2$ modified biochar had the greatest sorption capacity for both metals, $MgCl_2$ had the second highest sorption capacity, and unmodified biochar showed the lowest sorption capacity. One thing to note is that neither the Langmuir or Freundlich model fit the sorption data to a significant degree (R^2 <0.85). This may be due to the fact that the grinding of the biochar to obtain a specific size range led to significant variation between biochar placed in each triplicate sample. Furthermore, the small dose of biochar used to create the sorption isotherms (0.5 g/L, chosen so as to be able to control solution pH) may have further exacerbated the fact that the ground biochar particles were heterogeneous. It should also be noted that it is very likely that multiple sorption mechanisms were responsible for the observed isotherms. This means that the simple sorption models used to fit the data would be unable to completely explain the realized data.

While explaining mechanisms of sorption is not part of this research, possible reasons for the increased sorption capacity of the modified biochars may include increased ion exchange and surface complexation between magnesium minerals/surface functional groups on the biochar and the heavy metals in solution. These mechanisms may be increased, (assuming magnesium minerals were successfully impregnated on the modified biochar during pyrolysis), in the modified biochar due to increased magnesium mineral content and surface functional group content as compared to the unmodified biochar. In

the article by (Cui et al., 2016) it was found that both ion exchange and surface complexation were major contributors towards heavy metal sorption onto biochar (Cui et al., 2016). Thus, it is possible that these mechanisms may have contributed to increased copper and nickel sorption onto the modified biochars.

D. alaskensis growth was found to be unaffected by the presence of biochar for biochar doses ranging from 0.5 to 10.0 g/L (Table 17). This indicates that neither biochar, nor its soluble components, inhibits growth of *D. alaskensis*. While no inhibition of growth was expected, this was a necessary step before further testing with the biochar could be carried out, since some biochars, especially municipal sludge-derived biochars, have been shown to contain a significant amount of microbe-inhibiting heavy metals and polycyclic aromatic hydrocarbons (PAHs) (Kloss et al., 2012; Lu et al., 2012). In addition, as stated before, the amount of sulfate reduced and the amount of lactate converted to acetate agrees stoichiometrically with what is expected (Figure 7, Figure *10*, and Figure *11*). This means that all the electrons are accounted for throughout the 72-hour growth period, suggesting that the tested biochar does not contain any significant amount of labile carbon that can be accessed by *D. alaskensis* (an addition cell suspension with cells, biochar, and no lactate present also showed no sulfate reduction occurring). This is in agreement with the highly recalcitrant and aromatic nature of carbon in biochar, and with a study by Xu et al. (2016) that found that *Shewanella oneidensis* MR-1 could not use the carbon in biochar as a substitute for lactate for hematite reduction (Xu et al., 2016). It was found, however, that the 0.5 and 5.0 g/L biochar treatments resulted in lower total cell yields when compared to the control. This is strange, since this does not seem to be based on biochar concentration. While this cannot be ignored, it may be due to sampling biases (such as biochar size

fractionation) when withdrawing samples for qPCR into the needle, and also DNA extraction biases when extracting DNA from biochar containing samples.

For the copper inhibition growth experiment, the addition of biochar to copper containing media decreases the lag time for initiation of sulfate reduction by *D. alaskensis* for a copper concentration of 0.5 mg/L, which can be seen in both the sulfate and cell number data (Figure 15). The 1.0 mg/L copper experiment led to more ambiguous results (Figure 16). For this experiment, it appears that sulfate reduction took place at a similar rate regardless of whether biochar was present. However, there does appear to be a slight decrease in lag time based on cell number data. Furthermore, while the 0.5 mg/L copper experiment resulted in no statistical difference in total cell yield, the 1.0 mg/L copper experiment resulted in a greater total cell yield when biochar was present as compared to when it was not. This finding cannot be attributed to DNA extraction biases, as may be the case in the batch growth data, since the batch growth data showed total cell yield to decrease with biochar present. Copper, which is a known inhibitor of SRB, inhibits sulfate reduction by inactivating enzymes and nutrient transport systems (Nies, 1999). While biochar did not appear to decrease the copper concentration in solution, (see Appendix E: Initial Copper/Nickel Concentrations and Initial pH in Metal Inhibition Growth Studies) it may have decreased lag time by making copper ions less available to cells located on its surface. This would make it less energy intensive for *D. alaskensis*, which has to pump copper ions out through a ATPase efflux pumps encoded by genes such as the cop A and copB gene (Besaury et al., 2013; Nies, 1999). This need to expend energy to reduce copper inhibition by pumping can be seen in a noticeable decrease in total cell yield, as was stated above, through the statistical evidence from the 1.0 mg/L copper experiment.

Another possibility that needs to be considered is that biochar would provide a surface for cells to live on, encouraging growth. This is unlikely, however, since the *D. alaskensis* growth experiment (with no added copper) in the presence of varying doses of biochar showed no change in sulfate reduction rates, regardless of if biochar was present or not. Thus, surface area provided, and in turn, a surface, does not appear to be a factor. Furthermore, the 1.0 mg/L copper experiment likely showed no dependence on biochar addition due to the high copper concentration. This higher copper concentration may have masked whatever effect biochar has in these experiments. With little sorption capacity toward copper, (as found in the sorption experiment) the 1.0 mg/L of copper may have saturated the biochar, leaving all sorption sites occupied. Providing a greater dose of biochar, such as 5.0 g/L, may have a larger impact on lag time length as compared to a dose of 1.0 g/L due to additional copper sorption.

Cell suspension experiments are a way of quantifying the energetic bioenzymatic aspects of the metabolism of an organism in the absence of growth. In this study, the addition of biochar to resting cell suspensions containing *D. alaskensis*, lactate, sulfate, and HEPES buffer was found to significantly increase rates of sulfate reduction, irrespective of biochar dose (Figure 17). While Kappler et al. (2014) and Xu et al. (2016) have shown that biochar can act as an electron shuttle that stimulates electron transfer between bacteria and solid electron acceptors such as iron oxides, very few studies have looked at how biochar interacts with soluble electron acceptors, such as sulfate (Borchard, Prost, Kautz, Moeller, & Siemens, 2012; Kappler et al., 2014; Xu et al., 2016). One such study looked at the reduction of pentachlorophenol (PCP) by *Geobacter sulfurreducens* both with and without biochar present. In this study, it was found that various biochar

addition led up to a 24-fold enhancement in reductive dechlorination as compared to the control with no biochar (Yu et al., 2015). It was postulated that these enhancements were mostly due to the surface functional groups and electrical conductivity of the biochar leading to abiotic reduction of PCP by biochar which had been previously reduced by *G. sulfurreducens* (Yu et al., 2015). Furthermore, Cervantes et al. showed that *Desulfitobacterium* PCE1 was capable of coupling anthraquinone-2,6-disulphonate (AQDS, which is a humic analogue), reduction to lactate oxidation (Cervantes et al., 2002). This same study also showed that *Desulfovibrio* G11, a sulfate reducing bacterium, was able to use AQDS as a terminal electron acceptor during the oxidation of hydrogen (Cervantes et al., 2002). With the *Desulfovibrio* strain G11 capable of AQDS reduction, we hypothesize that *D. alaskensis* may also be able to couple lactate oxidation and biochar reduction. It needs to be noted that while AQDS is a soluble electron shuttle, biochar is a solid electron shuttle.

While the Yu et al. (2016) study is relevant towards finding out how biochar can act as a conduit for electron transfer and Cervantes et al. (2002) found that a SRB can reduce AQDS, the case with sulfate reduction by *D. alaskensis* is very different. This is due to the fact that biological sulfate reduction takes place within the cytoplasm of the cell (Keller et al., 2014). Furthermore, sulfate must first be activated by adenosine triphosphate (ATP) in the first step of biological sulfate reduction (see Figure 23) (Keller et al., 2014).

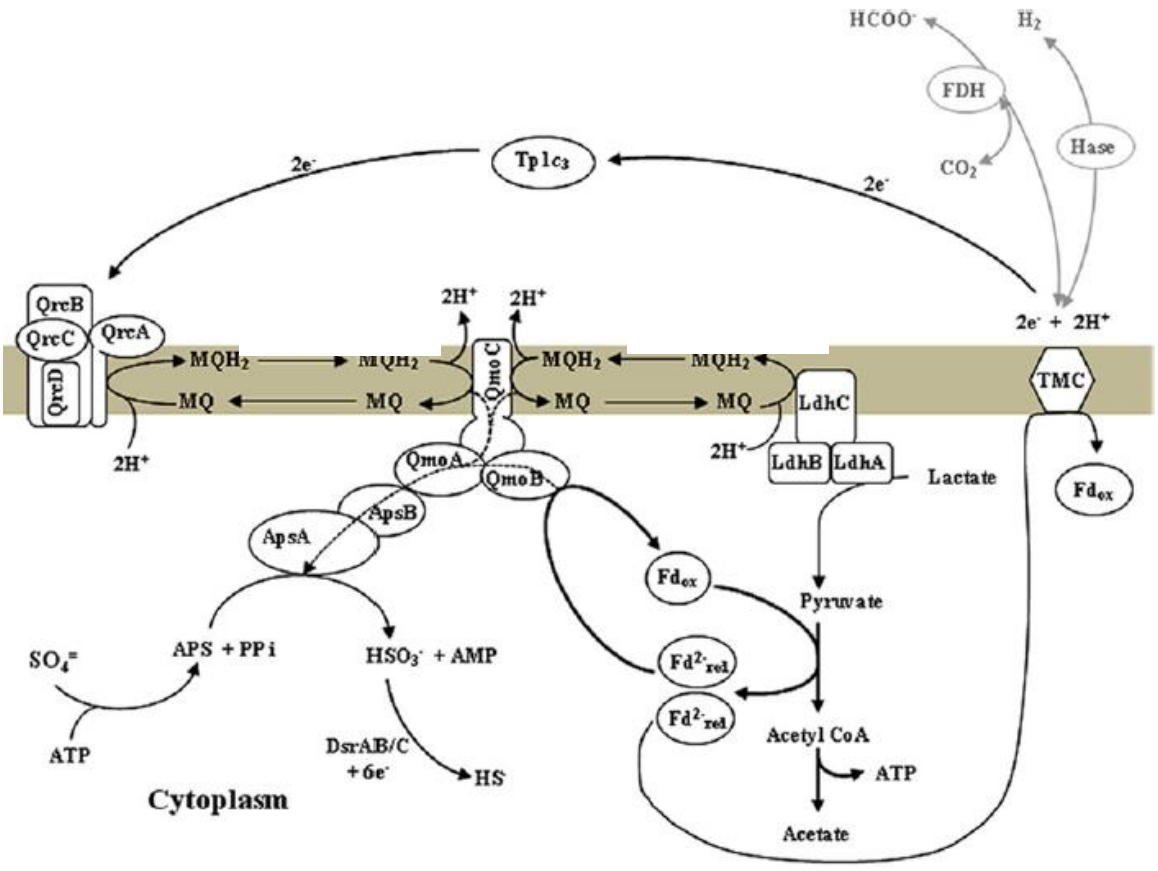

Figure 23: Proposed electron flow pathway for biological sulfate reduction from lactate in *D. alaskensis* G20 (Keller et al., 2014).

In addition, Figure 17, Figure *21*, and Figure *22* show that, based on stoichiometry, all the electrons that were needed to achieve the observed reduction in sulfate to sulfide in these cell suspensions roughly corresponds to the measured oxidation of lactate to acetate. This leads to the question of how can biochar increase sulfate reduction rates when sulfate reduction takes place within the cell and all electrons are accounted for?

One possible way that the addition of biochar may be able to increase sulfate reduction rates could be through the consumption of protons pumped out of the cell during the generation of the proton gradient. With biochar being an alkaline surface containing

redox active function groups, these surface functional groups would be able to accept protons, thus decreasing the strength of the proton gradient. Collapsing or decreasing the proton gradient would lead to a significant reduction in ATP synthesis. This would lead to the need for the cell to increase lactate turn over (and increase sulfate reduction) so as to maintain cell function by oxidative phosphorylation. Furthermore, this would also explain why biochar dose did not seem to affect the sulfate reduction rate. This would be due to the fact that the buffering capacity of the biochar was never reached during the experiment, even for the 0.5 g/L dose.

Another possibility involves biochar working as a battery that can provide electrons directly to the SRB so as to increase sulfate reduction. (Shi et al., 2016) The reason no sulfate reduction was observed in the abiotic series is due to the fact that sulfate must first be activated by ATP in the cell to adenosine phosphosulfate (APS) before it can be reduced (Keller et al., 2014). What leads to this not being very probable, however, is that all the electrons are accounted for during the reduction process of sulfate (through the analysis of lactate and acetate data). This leaves it as unlikely that electrons are coming from a different source other than from the oxidation of lactate, at least as long as alternative sources of an organic electron donor are available to the bacteria. Furthermore, biochar was not pre-reduced in the cell suspension, making it unlikely that *D. alaskensis* could have oxidized the biochar for sulfate reduction. It should be noted that, as shown in Figure 23 above, formate and hydrogen can also serve as extracellular electron donors during sulfate reduction. Thus, if biochar could act as a catalyst for e.g. hydrogen oxidation or directly provide electrons to electron accepting proteins on the surface of the cell, sulfate reduction would be possible. The hydrogen to proton redox potential is -414 millivolts, while the

formate to carbon dioxide redox potential is -432 millivolts. With unreduced humic acids having a redox potential between -120 ± 120 millivolts (similar to what would be expected for biochar due to its similarity with humics), however, the reduction of a more electro-negative electron acceptor is unlikely (Kluepfel, Keiluweit, Kleber, & Sander, 2014).

Outlook

This study looked to answer basic questions regarding sorption of heavy metals by modified biochar and the influence of biochar on sulfate reduction, specifically if it can act as an electron donor/acceptor. While modifying biochar by $MgCl_2$ and $Mg(OH)_2$ was found to increase sorption capacities towards nickel and copper, the mechanisms governing this sorption process are still unknown. To help identify possible mechanisms of sorption, scanning electron microscopy with energy dispersive X-ray spectroscopy (SEM/EDX) needs to be performed on biochar both before and after sorption. Through these techniques, changes in surface elemental composition, topography, and metal deposition information would be available to help determine surface chemistry for both modified and unmodified biochar. In addition, since the magnesium modified biochars showed much greater sorption capacities towards heavy metals, SRB should be grown in the presence of these biochars to see if the additional sorption capacity can alleviate heavy metal inhibition to a greater degree than unmodified biochar.

Future tests to determine if biochar can act as an electron donor/acceptor for sulfate reduction should utilize either reduced or oxidized biochar. One such test would be pre-reducing biochar with hydrogen and a palladium catalyst for use in a SRB cell suspension. Lactate could then be omitted from the cell suspension matrix so that if sulfate reduction is to occur, the electrons must come from the biochar, which could act as a battery to supply electrons (Shi et al., 2016). The other side of this test would be to use oxidized biochar in a cell suspension while omitting sulfate. By adding lactate to this suspension, the SRB would have to oxidize the lactate and reduce the biochar. This would determine the role biochar can play as an electron acceptor. While *D. alaskensis* may not be able to oxidize

or reduce biochar directly through its sulfate reduction metabolism, *D. alaskensis* is known to be able to reduce iron (Coleman, Hedrick, Lovley, White, & Pye, 1993; Lovley, Roden, Phillips, & Woodward, 1993). Thus, it may be possible for *D. alaskensis* to transfer electrons to biochar via the iron reduction system. Furthermore, soluble extracts from biochar should be tested in cell suspension experiments to determine if biochar has soluble electron shuttles that can be released from its surface. These findings could greatly impact AMD treatment through the use of biochar and SRB, either through addition to bioreactors, permeable reactive barriers, or packed columns.

Another area of future research that could have large implications in AMD treatment applications involves using electrodes to stimulate sulfate reduction. *D. alaskensis* has already been shown to be able to produce electrically-conductive nanoscale filaments capable of extracellular electron transfer to solid electron acceptors (Eaktasang et al., 2016). In another study, the SRB *Desulfovibrio ferrophilus* Strain IS5 has been shown to be able to accept electrons from a tin-doped oxide electrode while using sulfate as a terminal electron acceptor (Deng, Nakamura, Hashimoto, & Okamoto, 2015). Perhaps most importantly, though, is a study by Beese-Vasbender et al. (2015) that found *Desulfopila corrodens* strain IS4, a lithoautotrophic SRB was able to accept electrons from graphite and doped germanium cathodes (Beese-Vasbender, Nayak, Erbe, Stratmann, & Mayrhofer, 2015). This leads to the exciting possibility to directly supply electrons, instead of an organic electron donor, to autotrophic SRB to control sulfate reduction in engineered bioreactors.

Conclusion

This study looked to evaluate the potential of biochar to remove aqueous heavy metals from solution as well as the effect of biochar on microbial sulfate reduction in cell suspension assays and batch growth experiments. Overall, $Mg(OH)_2$ and $MgCl_2$ modified biochar were found to significantly increase sorptive capacity towards nickel and copper when compared to the unmodified control biochar. The mechanisms governing this sorptive process need to be further ascertained using SEM/EDX analysis. Furthermore, biochar was found to be able to relieve copper stress for a copper concentration of 0.5 mg/L. This relief of copper stress may be due to its above mentioned sorptive properties towards heavy metals. While biochar was shown to increase the extent of sulfate reduction by *Desulfovibrio alaskensis* up to 4-fold in suspension assays, the reason behind this finding is currently unknown. Further testing utilizing reduced and/or oxidized biochar is need to help discern the underlying process that governs this increase. In conclusion, biochar shows great promise as an additive material in permeable reactive barriers and packed columns for the treatment of AMD due to its ability to sorb heavy metals and increase sulfate reduction rates.

Appendix A: Swiss Biochar Properties

Table 23: Swiss biochar physical properties. Swiss biochar was used as the control biochar for the sorption experiments.

BET Surface area [m^2/g]	pH	C content [% mass]	N content [% mass]	H content [% mass]	O content [% mass]	S content [% mass]	Ni [g/ton]	Cu [g/ton]	Fe [mg/kg]	Zi [g/ton]	Cd [g/ton]	Mg [mg/kg]	Ca [mg/kg]	K [mg/kg]	Na [mg/kg]	Si [mg/kg]
231.9	8.0	73.2	0.64	1.03	5.7	0.06	8	16	2700	45	< 0.2	3300	49000	8400	830	22000

Appendix B: Nonlinear Regression Example for Nickel Sorption onto $MgCl_2$ Modified Biochar

-Langmuir

Table 24 below shows the Microsoft Excel spreadsheet used to perform nonlinear regression for the $MgCl_2$ modified biochar sorbing nickel based on the Langmuir model. Each part of the table will be explained below, along with sample calculations.

Table 24: Langmuir fit using nonlinear regression. SS stands for sum of squares.

KL [L/mg]	**0.0287**			
Qm [mg/g]	**16.1**			
Langmuir Nonlinear Regression				
Average Final Ni Conc. [mg/L]	Q Predicted [mg/g]	Q Actual [mg/g]	SS Residual [mg^2/g^2]	SS Total [mg^2/g^2]
0.00	---	---	---	---
8.58	3.19	3.08	0.01	24.51
18.23	5.54	3.87	2.77	17.31
27.13	7.06	6.46	0.35	2.46
36.50	8.24	9.31	1.14	1.64
45.32	9.11	11.36	5.06	11.08
55.12	9.87	10.84	0.94	7.89
66.60	10.58	9.43	1.32	1.96
76.43	11.07	9.90	1.37	3.48
		Sum:	**12.96**	**70.32**
		Q avg [mg/g]	8.03	
		R^2 [ ]	0.82	

- Average Final Ni Conc.: Represents the actual final nickel concentration found after 48 hours of interaction time. It is the average of the triplicate readings.

- Q Predicted: This is a prediction based on the KL value, Qm value, and the actual average final Ni concentration. This is calculated using Equation 3. A sample calculation for the 8.58 mg/L final nickel concentration line is shown below.

$$Q = \frac{Qm * KL * Cf}{(1 + KL * Cf)} = \frac{16.1\ \frac{mg}{g} * 0.0287\ \frac{L}{mg} * 8.58\ \frac{mg}{L}}{(1 + 0.0287\ \frac{mg}{g} * 8.58\ \frac{mg}{L})} = 3.19\ \frac{mg}{g}$$

- Q Actual: This represents the actual average sorption capacity of the triplicate samples based on the initial and final nickel concentration along with the dose of biochar used. This comes from the use of Equation 2.
- SS Residual: This is the sum of squares residual. This is represented by the equation below. An example calculation for the 8.58 mg/L final nickel concentration is also included.

$$SS\ Residual$$
$$= \sum (Q\ Actual - Q\ Predicted)^2$$
$$= (3.08\ \frac{mg}{g} - 3.19\ \frac{mg}{g})^2 + \cdots$$

- Q avg: Is the average of all the Q Actuals. This represents the average sorption capacity of the biochar across all tested nickel concentrations.
- SS Total: This is the total sum of squares. This is represented by the equation below. An example calculation for the 8.58 mg/L final nickel concentration is also included.

$$SS\ Total = \sum (Q\ Actual - Q\ avg)^2 = \left(3.08\ \frac{mg}{g} - 8.03\ \frac{mg}{g}\right)^2 + \cdots$$

- R^2: This represent the degree of fit for the KL and Qm value. This is calculate as shown below.

$$R^2 = \left(1 - \frac{SS\ Residual}{SS\ Total}\right) = \left(1 - \frac{12.96\ \frac{mg^2}{g^2}}{70.32\ \frac{mg^2}{g^2}}\right) = 0.82\ [\,]$$

The solver function in Microsoft Excel could then be used to maximize the R^2 value. This was done by setting the KL and Qm values as the variables, with maximizing the R^2 value as the target.

-Freundlich

Table 25 below shows the Microsoft Excel spreadsheet used to perform nonlinear regression for the $MgCl_2$ modified biochar sorbing nickel based on the Freundlich model. Each part of the table will be explained below, along with sample calculations.

Table 25: Freundlich fit using nonlinear regression. SS stands for sum of squares.

F [mg/g]	**1.298**			
n [ ]	**0.502**			
Freundlich Nonlinear Regression				
Average Final Ni Conc. [mg/L]	Q Predicted [mg/g]	Q Actual [mg/g]	SS Residual [mg^2/g^2]	SS Total [mg^2/g^2]
0.00	---	---	---	---
8.58	3.81	3.08	0.54	24.51
18.23	5.57	3.87	2.87	17.31
27.13	6.79	6.46	0.11	2.46
36.50	7.88	9.31	2.04	1.64
45.32	8.79	11.36	6.62	11.08
55.12	9.69	10.84	1.32	7.89
66.60	10.66	9.43	1.51	1.96
76.43	11.42	9.90	2.32	3.48
		Sum:	**17.32**	**70.32**
		Q avg [mg/g]	8.03	
		R^2 [ ]	0.75	

- Average Final Ni Conc.: As explained above.
- Q Predicted: This is a prediction based on the F value, n value, and the actual average final Ni concentration. This is calculated using Equation 4. A sample calculation for the 8.58 mg/L final nickel concentration line is shown below.

$$Q = F * Cf^n = 1.298 \frac{mg}{g} * \left(8.58 \frac{mg}{L}\right)^{0.502} = 3.82 \frac{mg}{g}$$

- Q Actual: As explained above.
- SS Residual: As explained above.
- Q avg: As explained above.

- SS Total: As explained above.
- R^2: This represent the degree of fit for the F and n value. This is calculate as shown below.

$$R^2 = \left(1 - \frac{SS\ Residual}{SS\ Total}\right) = \left(1 - \frac{17.32\ \frac{mg^2}{g^2}}{70.32\ \frac{mg^2}{g^2}}\right) = 0.75\ [\,]$$

The solver function in Microsoft Excel could then be used to maximize the R^2 value. This was done by setting the F and N values as the variables, with maximizing the R^2 value as the target.

Appendix C: *D. alaskensis* Log Growth Figures

-D. alaskensis Growth in Presence of Biochar

The qPCR results depicting the number of *D. alaskensis* cells per milliliter during log phase growth of this experiment can be seen in Figure 24, Figure 25, Figure 26, Figure 27, and Figure 28 below. From these graphs, the growth rate could be found for each series by plotting the results on a log scale for cell number per milliliter. A linear line could then be fit to the data, from which the specific growth rate could be determined.

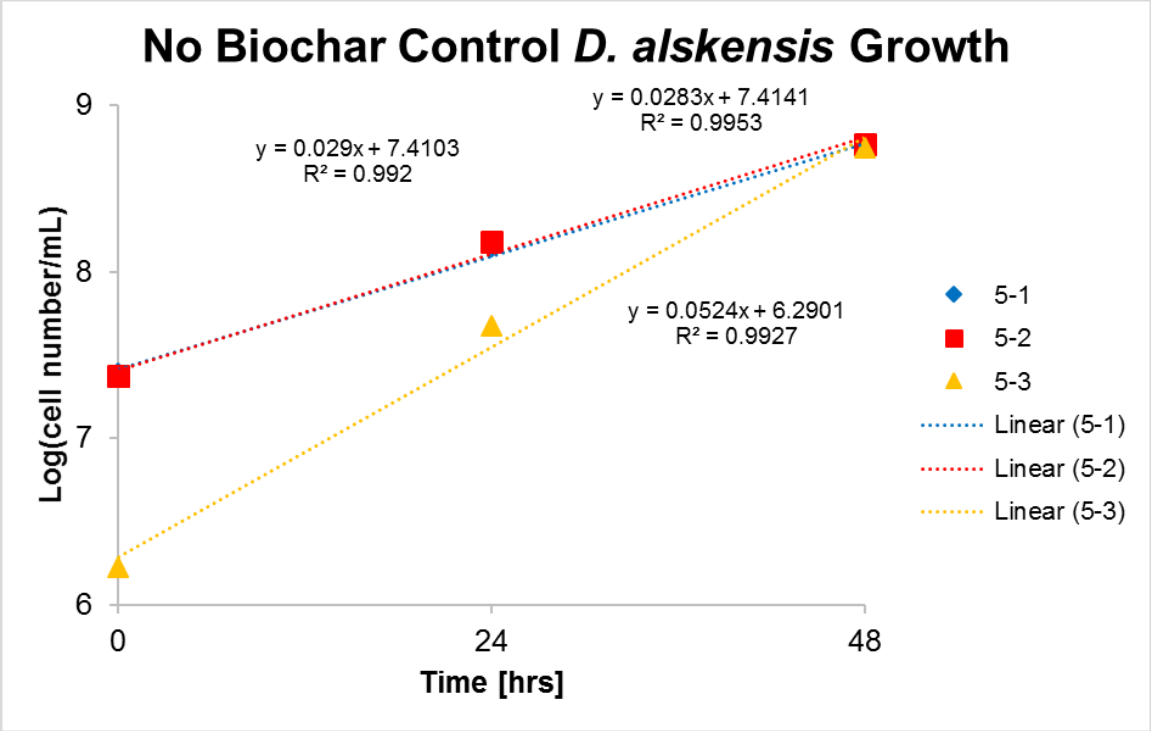

Figure 24: Growth of cells for triplicate control samples (no biochar) during log growth. Dotted lines represent linear fits.

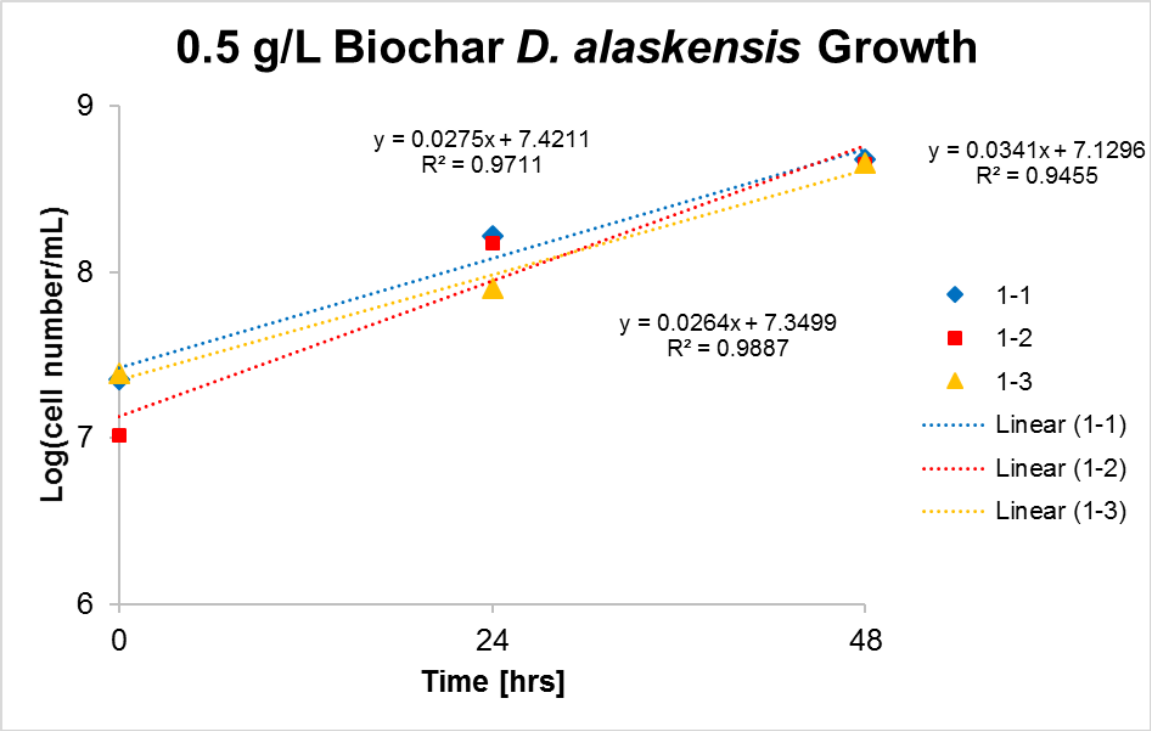

Figure 25: Growth of cells for triplicate 0.5 g/L dose biochar samples during log growth. Dotted lines represent linear fits.

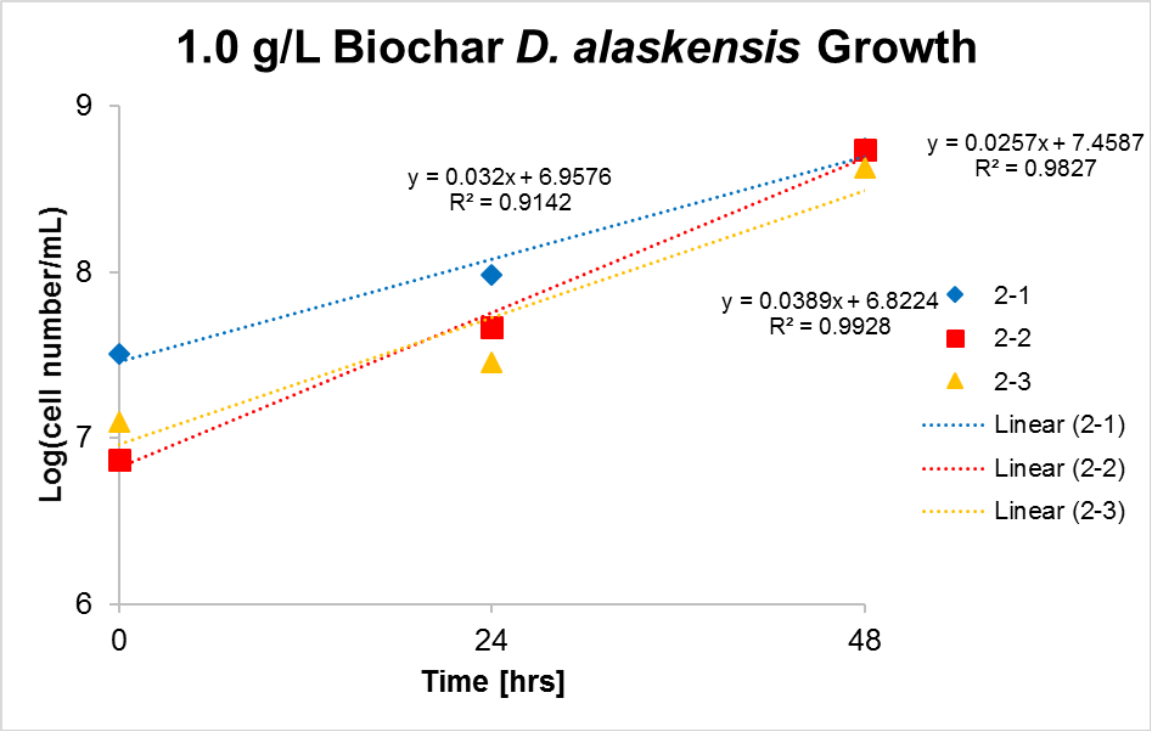

Figure 26: Growth of cells for triplicate 1.0 g/L dose biochar samples during log growth. Dotted lines represent linear fits.

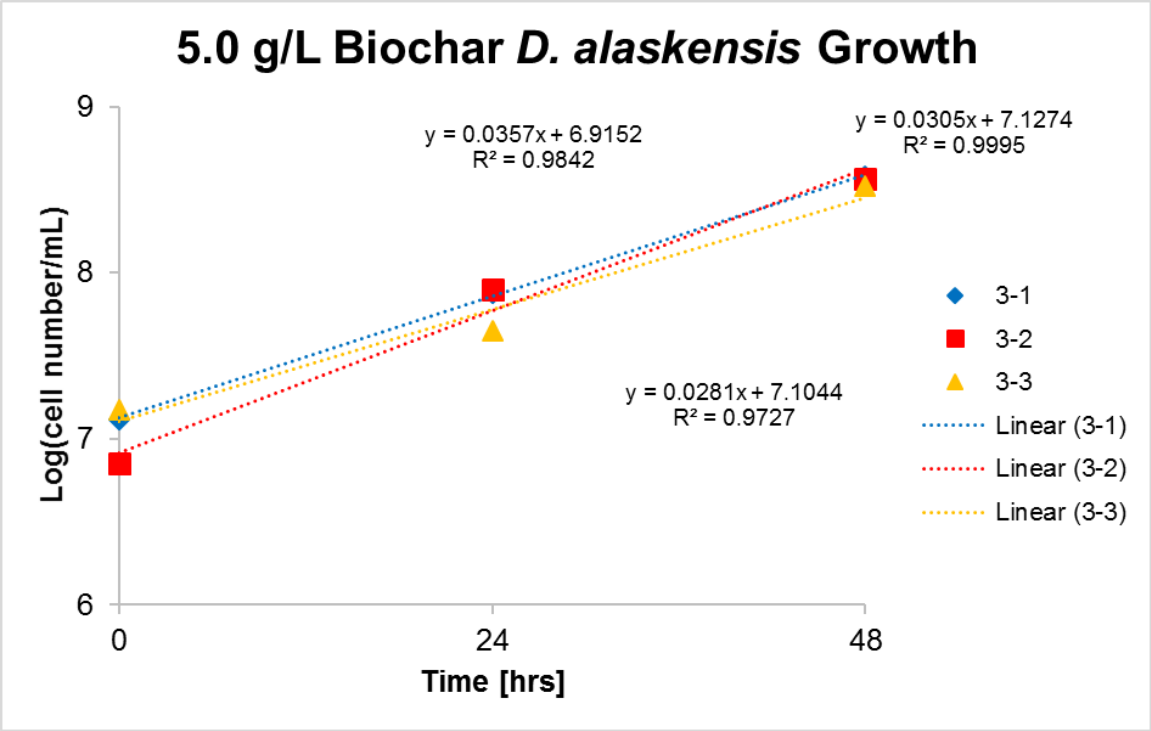

Figure 27: Growth of cells for triplicate 5.0 g/L dose biochar samples during log growth. Dotted lines represent linear fits.

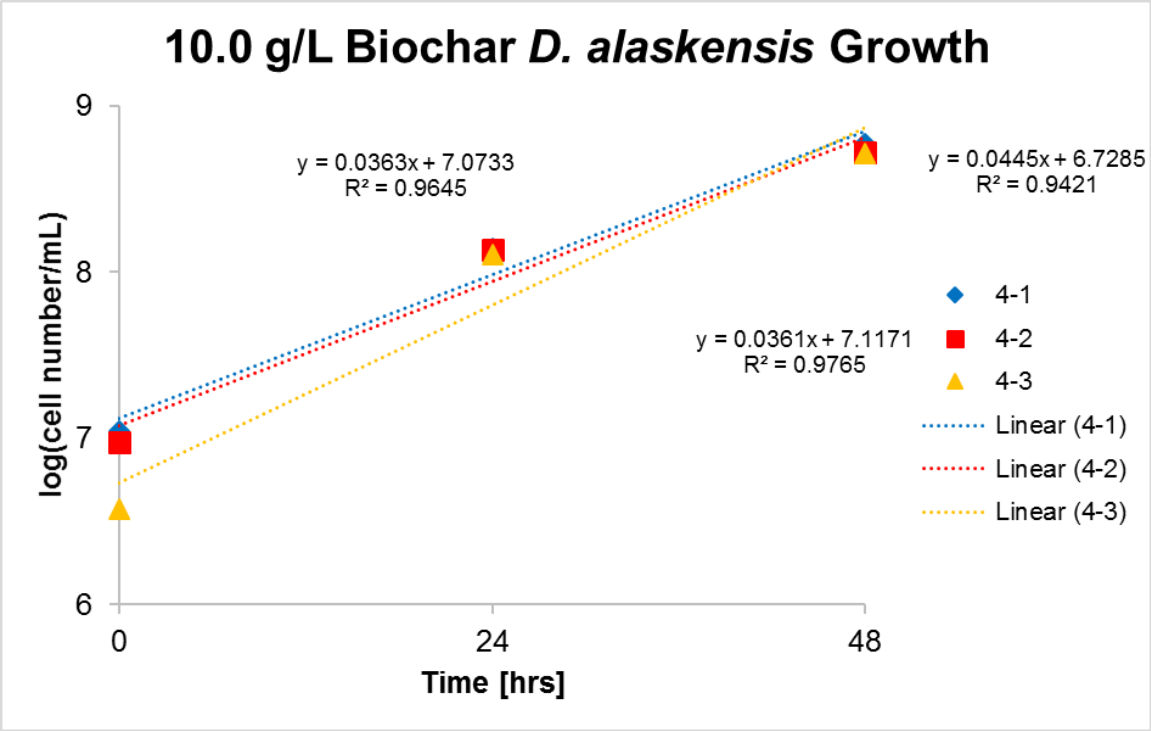

Figure 28: Growth of cells for triplicate 10.0 g/L dose biochar samples during log growth. Dotted lines represent linear fits.

-D. alaskensis Metal Inhibition Growth

The qPCR results depicting the number of *D. alaskensis* cells per milliliter during log phase growth of the 0.5 mg/L copper experiments can be seen in Figure 29, Figure 30, Figure 31 . From these graphs, the growth rate could be found for each series by plotting the results on a log scale for cell number per milliliter. A linear line could then be fit to the data, from which the specific growth rate could be determined.

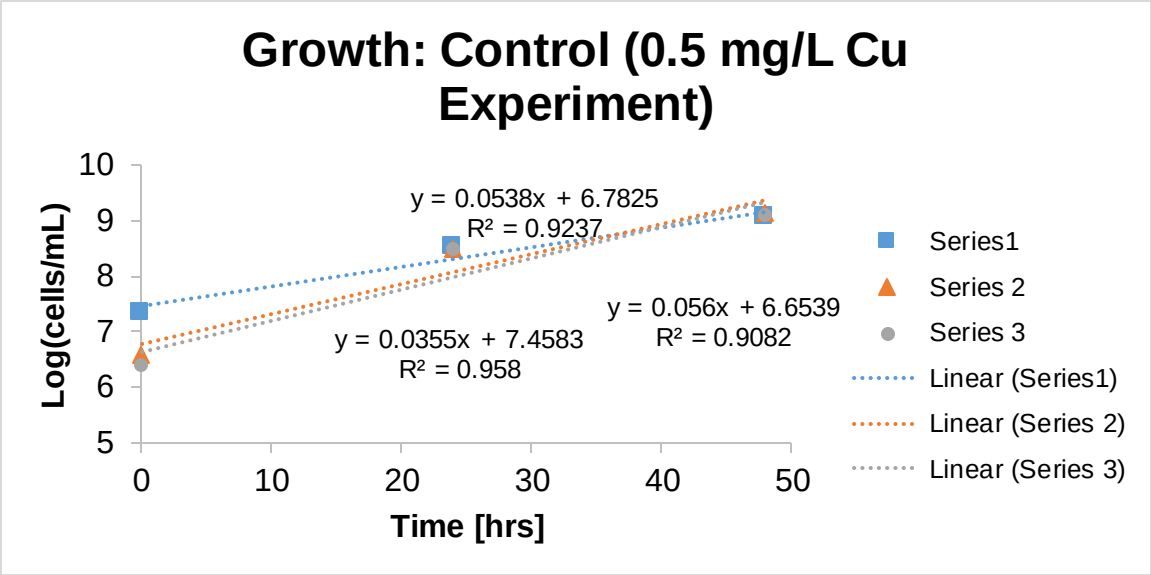

Figure 29: Growth of *D. alaskensis* for triplicate control series (0.5 mg/L copper experiment) during log growth. Control series contained no copper or biochar. Dotted lines represent linear fits.

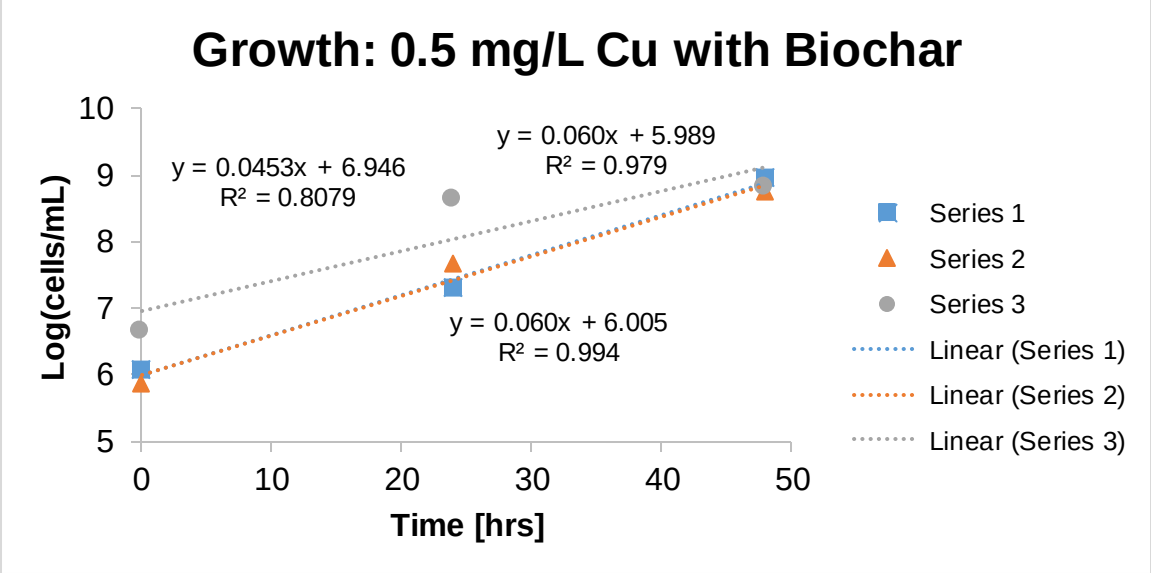

Figure 30: Growth of *D. alaskensis* for triplicate 1.0 g/L dose biochar samples containing 0.5 mg/L copper during log growth. Dotted lines represent linear fits.

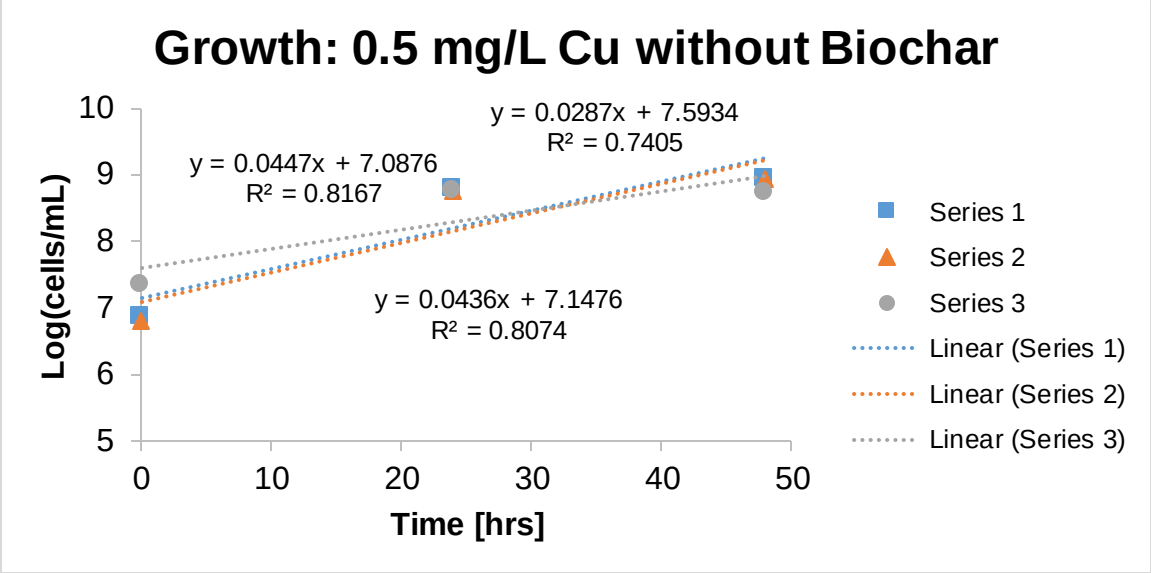

Figure 31: Growth of *D. alaskensis* for triplicate 0.5 mg/L copper samples during log growth. No biochar was added to this series. Dotted lines represent linear fits.

The qPCR results depicting the number of *D. alaskensis* cells per milliliter during log phase growth of the 1.0 mg/L copper experiments can be seen in Figure 32, Figure 33, and Figure 34. From these graphs, the growth rate could be found for each series by plotting the results on a log scale for cell number per milliliter.

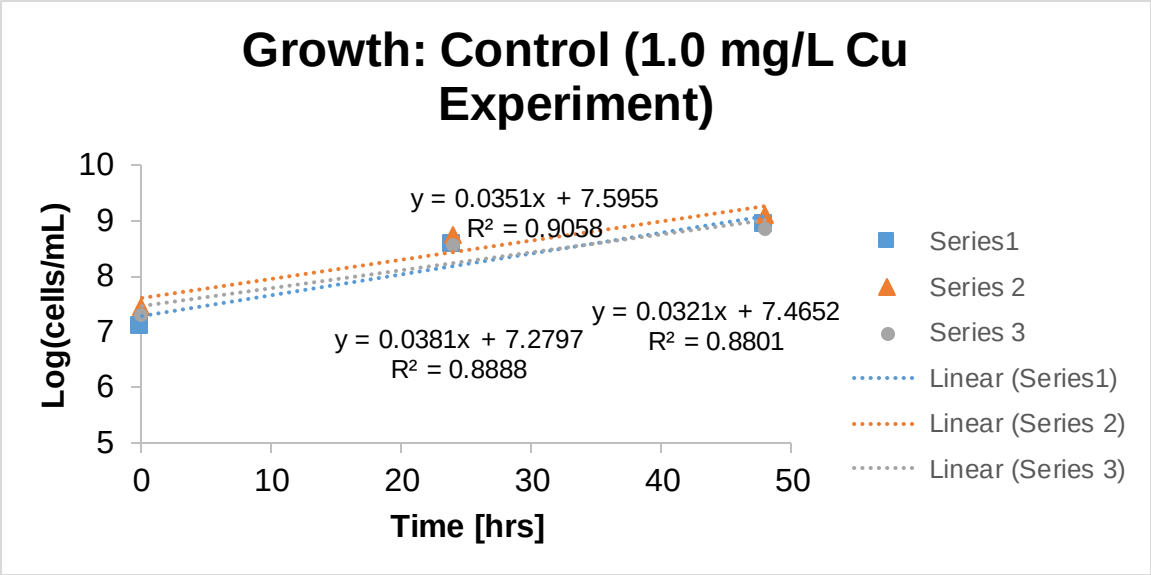

Figure 32: Growth of *D. alaskensis* for triplicate control series (0.5 mg/L copper experiment) during log growth. Control series contained no copper or biochar. Dotted lines represent linear fits.

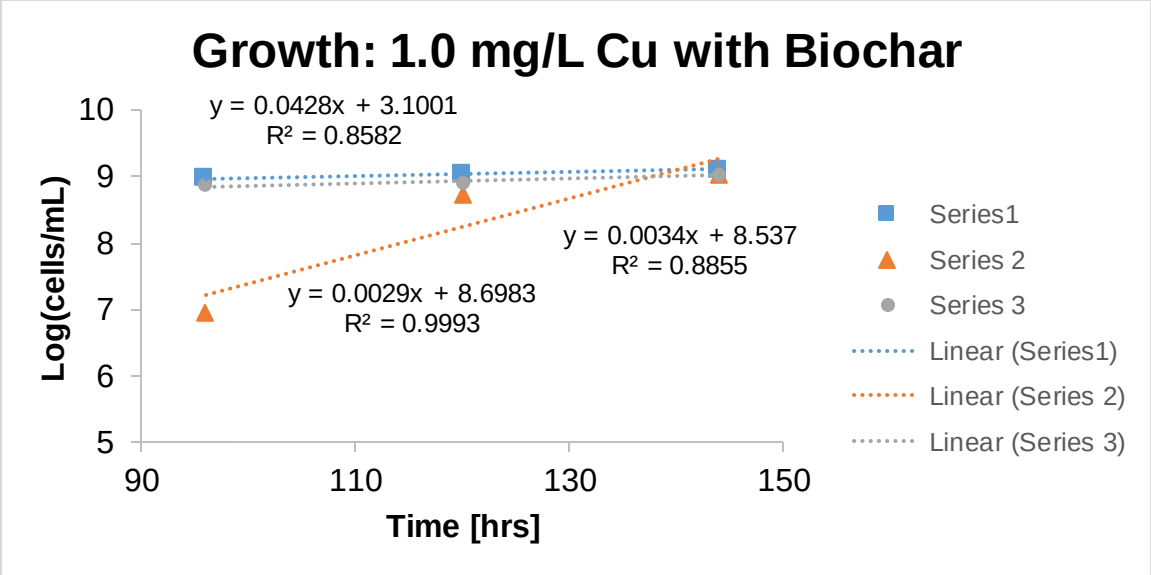

Figure 33: Growth of *D. alaskensis* for triplicate 1.0 g/L dose biochar samples containing 1.0 mg/L copper during log growth. Dotted lines represent linear fits.

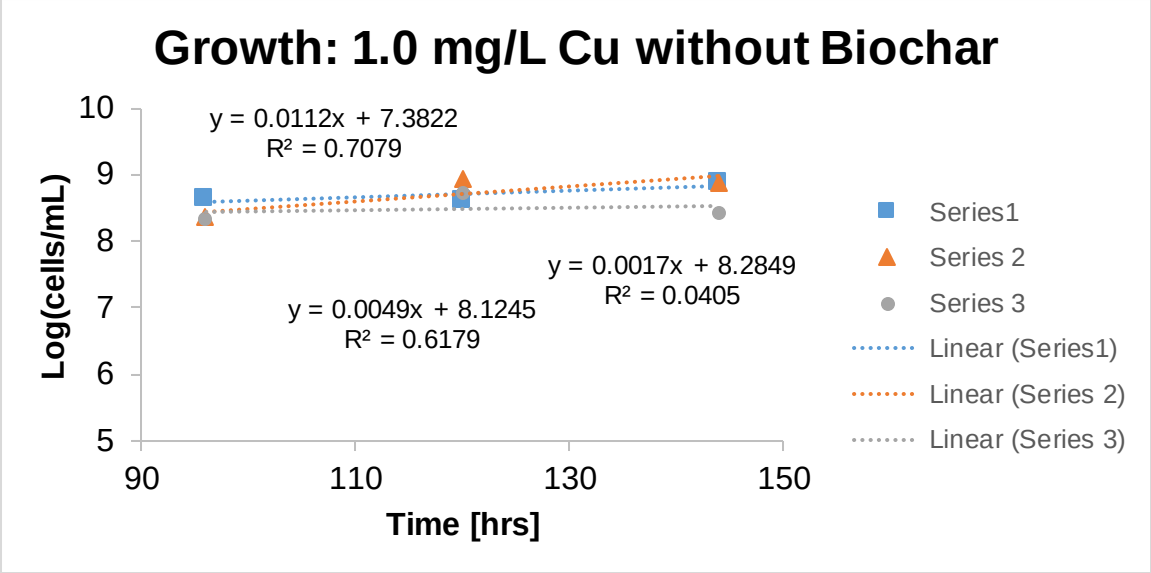

Figure 34: *Growth* of D. alaskensis *for triplicate 1.0* mg/L copper samples during log growth. No biochar was added to this series. Dotted lines represent linear fits.

Appendix D: Abiotic Copper Metal Inhibition Control

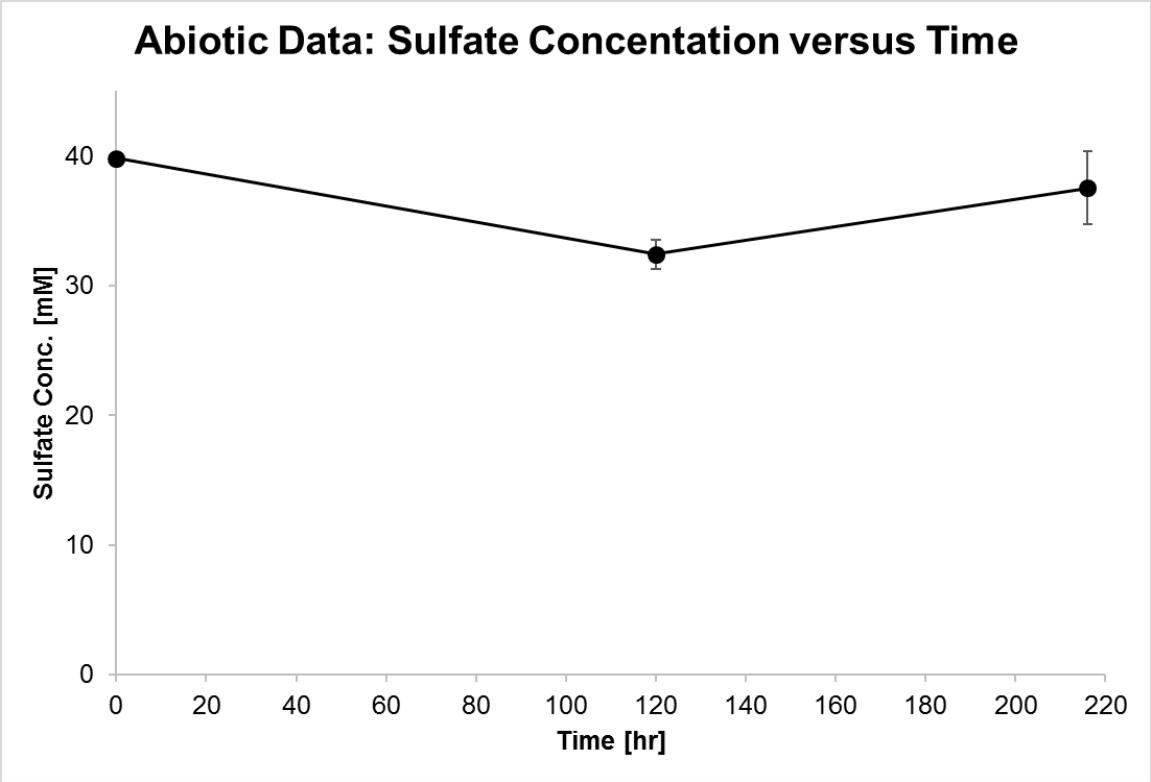

Figure 35: Sulfate concentration versus time for the abiotic series containing 1.0 g/L biochar, 2.5 mg/L copper, and no cells. Error bars represent the standard deviation between triplicate samples.

Appendix E: Initial Copper/Nickel Concentrations and Initial pH in Metal Inhibition Growth Studies

-Copper Inhibition Study

Table 26: Expected and actual initial copper concentrations in the copper inhibition growth studies.

Triplicate Sample	Expected Cu Conc. [mg/L]	Actual Cu Conc. [mg/L]	Avg. Cu Conc. [mg/L]
1-1	0 (Control)	0.02	0.008
1-2	0 (Control)	0.00	
1-3	0 (Control)	0.00	
2-1	0.5	0.27	0.248
2-2	0.5	0.27	
2-3	0.5	0.21	
3-1	2.5	1.94	2.013
3-2	2.5	1.91	
3-3	2.5	2.19	
4-1	5.0	4.13	4.296
4-2	5.0	4.44	
4-3	5.0	4.32	
5-1	0.5	0.45	0.309
5-2	0.5	0.24	
5-3	0.5	0.24	
6-1	2.5	1.88	2.023
6-2	2.5	2.12	
6-3	2.5	2.06	
7-1	5.0	4.53	4.489
7-2	5.0	4.41	
7-3	5.0	4.53	
8-1	2.5	2.12	2.226
8-2	2.5	2.40	
8-3	2.5	2.16	
9-1*	1.0	0.285326	0.285
9-2*	1.0	0.350154	
9-3*	1.0	0.220498	
10-1*	1.0	0.220498	0.264
10-2*	1.0	0.285326	
10-3*	1.0	0.285326	
*Were not acidified			

Notes: 9 and 10 series were not acidified before FAAS measurements. It is expected that these values reflect a slightly smaller copper concentration than would be seen if they were acidified. In addition, 9 and 10 series triplicate samples are from an additional experiment that was performed as explained in the methods. The control triplicate samples from this additional experiment was not included in this table since they were identical to the 1 control triplicate samples from the first experiment, with no measurable copper observed.

Table 27: Initial pH of triplicate samples in the copper inhibition growth study. 9 and 10 series triplicate samples are from an additional experiment that was performed as explained in the methods.

Triplicate Sample	Expected pH	Actual pH	Avg. pH
1-1	6.5	6.51	6.50
1-2	6.5	6.49	
1-3	6.5	6.49	
2-1	6.5	6.68	6.68
2-2	6.5	6.70	
2-3	6.5	6.65	
3-1	6.5	6.65	6.66
3-2	6.5	6.68	
3-3	6.5	6.65	
4-1	6.5	6.65	6.65
4-2	6.5	6.66	
4-3	6.5	6.65	
5-1	6.5	6.47	6.47
5-2	6.5	6.46	
5-3	6.5	6.47	
6-1	6.5	6.47	6.46
6-2	6.5	6.46	
6-3	6.5	6.45	
7-1	6.5	6.46	6.46
7-2	6.5	6.45	
7-3	6.5	6.46	
8-1	6.5	6.64	6.64
8-2	6.5	6.64	
8-3	6.5	6.63	
9-1*	6.5	6.67	6.70
9-2*	6.5	6.70	
9-3*	6.5	6.72	
10-1*	6.5	6.56	6.51
10-2*	6.5	6.47	
10-3*	6.5	6.51	

-Nickel Inhibition Study

Table 28: Expected and actual initial copper concentrations in the nickel inhibition growth studies.

Triplicate Sample	Expected Cu Conc. [mg/L]	Actual Cu Conc. [mg/L]	Avg. Cu Conc. [mg/L]
1-1	0 (Control)	0.00	0.000
1-2	0 (Control)	0.00	
1-3	0 (Control)	0.00	
2-1	20	18.75	18.693
2-2	20	18.75	
2-3	20	18.58	
3-1	60	56.74	56.408
3-2	60	56.74	
3-3	60	55.75	
4-1	120	112.49	110.180
4-2	120	110.51	
4-3	120	107.54	
5-1	20	18.25	17.265
5-2	20	17.10	
5-3	20	16.44	
6-1	60	56.28	55.507
6-2	60	55.29	
6-3	60	54.96	
7-1	120	113.47	113.474
7-2	120	114.46	
7-3	120	112.49	
8-1	60	57.23	55.914
8-2	60	56.74	
8-3	60	53.77	

Table 29: Initial pH of triplicate samples in the nickel inhibition growth study.

Triplicate Sample	Expected pH	Actual pH	Avg. pH
1-1	6.5	6.45	6.43
1-2	6.5	6.42	
1-3	6.5	6.42	
2-1	6.5	6.61	6.60
2-2	6.5	6.60	
2-3	6.5	6.59	
3-1	6.5	6.53	6.54
3-2	6.5	6.55	
3-3	6.5	6.54	
4-1	6.5	6.53	6.53
4-2	6.5	6.53	
4-3	6.5	6.53	
5-1	6.5	6.39	6.38
5-2	6.5	6.37	
5-3	6.5	6.37	
6-1	6.5	6.34	6.33
6-2	6.5	6.33	
6-3	6.5	6.32	
7-1	6.5	6.32	6.32
7-2	6.5	6.32	
7-3	6.5	6.32	
8-1	6.5	6.54	6.54
8-2	6.5	6.52	
8-3	6.5	6.55	

Appendix F: Nickel Inhibition of *D. alaskensis* Growth Sulfate Measurements

Figure 36, Figure 37, and Figure 38 below depict the sulfate data obtained from the nickel inhibition growth experiment. While the 20 mg/L nickel concentration experiments appear to have worked, all other nickel concentrations, including the control, had greatly depressed sulfate concentrations. The cause of this is unknown but is suspected to be due to nickel interference with ion chromatography measurements. Assuming the 20 mg/L nickel experiments were unaffected, 20 mg/L of nickel did not seem to affect growth of *D. alaskensis*. With the 60 and 120 mg/L nickel sulfate data being greatly depressed, it is unclear whether or not biochar can relieve nickel inhibition.

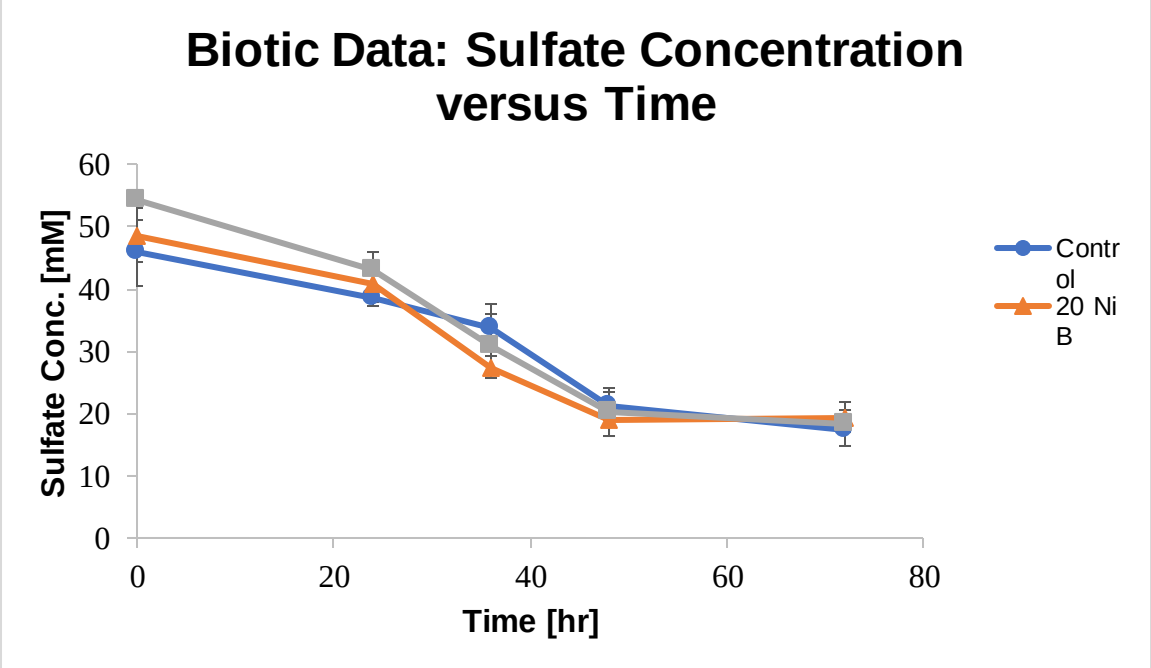

Figure 36: Sulfate concentration versus time for the nickel toxicity *D. alaskensis* growth experiment in the presence of 1.0 g/L biochar and copper. 20 Ni represents 20 mg/L copper concentration. Series that contained biochar are represented with a B. Error bars represent the standard deviation between triplicate samples.

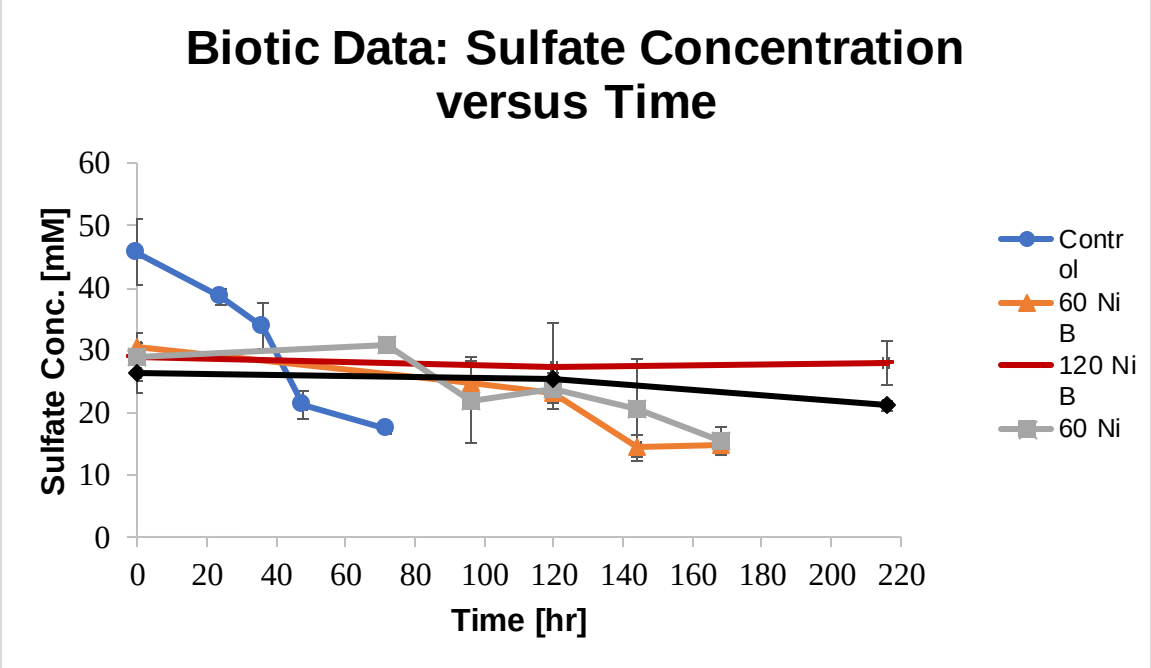

Figure 37: Sulfate concentration versus time for the nickel toxicity *D. alaskensis* growth experiment in the presence of 1.0 g/L biochar and copper. 60 Ni represents 60 mg/L copper concentration. Series that contained biochar are represented with a B. Error bars represent the standard deviation between triplicate samples.

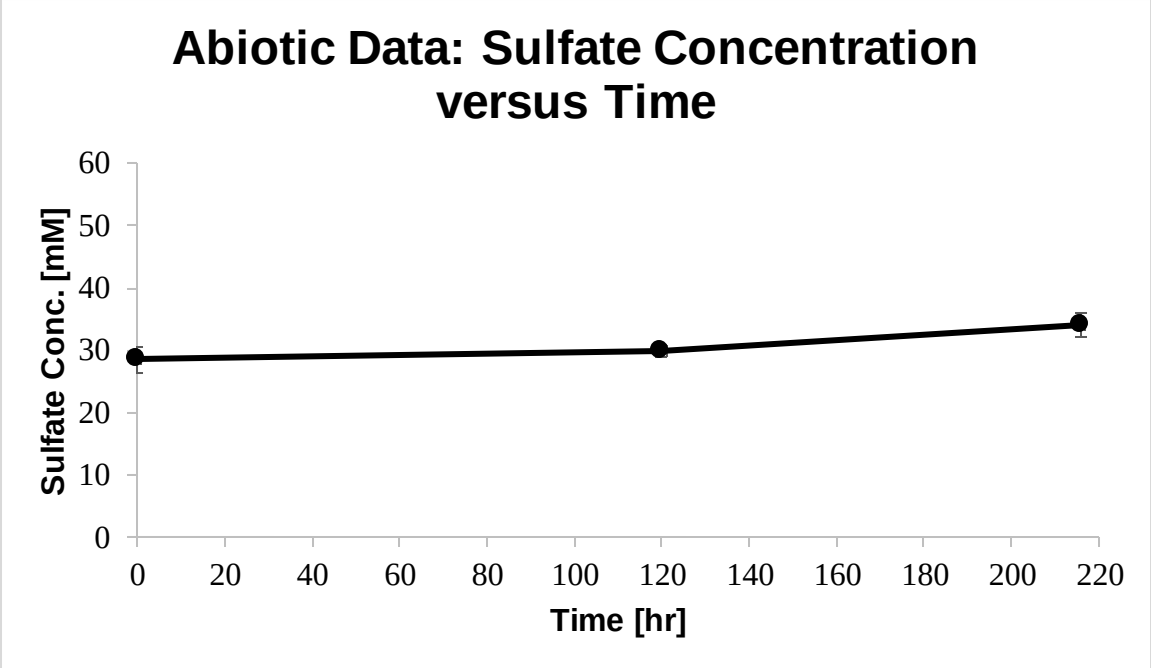

Figure 38: Sulfate concentration versus time for the nickel toxicity *D. alaskensis* growth experiment in the presence of 1.0 g/L biochar and copper. This represents the abiotic control series. This series contained 60 mg/L nickel, 1.0 g/L biochar, and no cells. Error bars represent the standard deviation between triplicate samples.

References

Ahmad, M., Rajapaksha, A. U., Lim, J. E., Zhang, M., Bolan, N., Mohan, D., et al. (2014). Biochar as a sorbent for contaminant management in soil and water: A review. *Chemosphere, 99*, 19-33.

Babel, S., & Kurniawan, T. A. (2004). Cr(VI) removal from synthetic wastewater using coconut shell charcoal and commercial activated carbon modified with oxidizing agents and/or chitosan. *Chemosphere, 54*(7), 951-967.

Barber, J., Parker, H., Frost, D., Hartley, J., White, T., Martin, C., Sterrett, R. (2014). Twin Metals Minnesota Project: Technical Report on Pre-feasibility Study. Duluth Metals Corp.

Beese-Vasbender, P. F., Nayak, S., Erbe, A., Stratmann, M., & Mayrhofer, K. J. J. (2015). Electrochemical characterization of direct electron uptake in electrical microbially influenced corrosion of iron by the lithoautotrophic SRB Desulfopila corrodens strain IS4. *Electrochimica Acta, 167*, 321-329.

Beesley, L., Moreno-Jimenez, E., Gomez-Eyles, J. L., Harris, E., Robinson, B., & Sizmur, T. (2011). A review of biochars' potential role in the remediation, revegetation and restoration of contaminated soils. *Environmental Pollution, 159*(12), 3269-3282.

Besaury, L., Marty, F., Buquet, S., Mesnage, V., Muyzer, G., & Quillet, L. (2013). Culture-Dependent and Independent Studies of Microbial Diversity in Highly Copper-Contaminated Chilean Marine Sediments. *Microbial Ecology, 65*(2), 311-324.

Bigham, J. M., & Nordstrom, D. K. (2000). Iron and aluminum hydroxysulfates from acid sulfate waters. *Sulfate Minerals - Crystallography, Geochemistry and Environmental Significance, 40*, 351-403.

Borchard, N., Prost, K., Kautz, T., Moeller, A., & Siemens, J. (2012). Sorption of copper (II) and sulphate to different biochars before and after composting with farmyard manure. *European Journal of Soil Science, 63*(3), 399-409.

Brandis, A., & Thauer, R. K. (1981). GROWTH OF DESULFOVIBRIO SPECIES ON HYDROGEN AND SULFATE AS SOLE ENERGY-SOURCE. *Journal of General Microbiology, 126*(SEP), 249-252.

Bureau of Business and Economic Research. (2012). The Economic Impact of Ferrous and Non-Ferrous Mining. Duluth: Labovitz School of Business and Economics, University of Minnesota Duluth.

Caraballo, M. A., Macias, F., Rotting, T. S., Nieto, J. M., & Ayora, C. (2011). Long term remediation of highly polluted acid mine drainage: A sustainable approach to restore the environmental quality of the Odiel river basin. *Environmental Pollution, 159*(12), 3613-3619.

Cervantes, F. J., de Bok, F. A. M., Tuan, D. D., Stams, A. J. M., Lettinga, G., & Field, J. A. (2002). Reduction of humic substances by halorespiring, sulphate-reducing and methanogenic microorganisms. *Environmental Microbiology, 4*(1), 51-57.

Chen, B. L., Chen, Z. M., & Lv, S. F. (2011). A novel magnetic biochar efficiently sorbs organic pollutants and phosphate. *Bioresource Technology, 102*(2), 716-723.

Coleman, M. L., Hedrick, D. B., Lovley, D. R., White, D. C., & Pye, K. (1993). REDUCTION OF FE(III) IN SEDIMENTS BY SULFATE-REDUCING BACTERIA. *Nature, 361*(6411), 436-438.

Cordruwisch, R. (1985). A QUICK METHOD FOR THE DETERMINATION OF DISSOLVED AND PRECIPITATED SULFIDES IN CULTURES OF SULFATE-REDUCING BACTERIA. *Journal of Microbiological Methods, 4*(1), 33-36.

Cui, X. Q., Fang, S. Y., Yao, Y. Q., Li, T. Q., Ni, Q. J., Yang, X. E., et al. (2016). Potential mechanisms of cadmium removal from aqueous solution by Canna indica derived biochar. *Science of the Total Environment, 562*, 517-525.

Deng, X., Nakamura, R., Hashimoto, K., & Okamoto, A. (2015). Electron Extraction from an Extracellular Electrode by Desulfovibrio ferrophilus Strain IS5 Without Using Hydrogen as an Electron Carrier. *Electrochemistry, 83*(7), 529-531.

Eaktasang, N., Kang, C. S., Lim, H., Kwean, O. S., Cho, S., Kim, Y., et al. (2016). Production of electrically-conductive nanoscale filaments by sulfate-reducing bacteria in the microbial fuel cell. *Bioresource Technology, 210*, 61-67.

Ennis, C. J., Evans, A. G., Islam, M., Ralebitso-Senior, T. K., & Senior, E. (2012). Biochar: Carbon Sequestration, Land Remediation, and Impacts on Soil Microbiology. *Critical Reviews in Environmental Science and Technology, 42*(22), 2311-2364.

Evangelou, V. P., & Zhang, Y. L. (1995). A REVIEW - PYRITE OXIDATION MECHANISMS AND ACID-MINE DRAINAGE PREVENTION. *Critical Reviews in Environmental Science and Technology, 25*(2), 141-199.

Fang, C., Zhang, T., Li, P., Jiang, R. F., & Wang, Y. C. (2014). Application of Magnesium Modified Corn Biochar for Phosphorus Removal and Recovery from Swine Wastewater. *International Journal of Environmental Research and Public Health, 11*(9), 9217-9237.

Fellet, G., Marchiol, L., Delle Vedove, G., & Peressotti, A. (2011). Application of biochar on mine tailings: Effects and perspectives for land reclamation. *Chemosphere, 83*(9), 1262-1267.

Gul, S., Whalen, J. K., Thomas, B. W., Sachdeva, V., & Deng, H. Y. (2015). Physico-chemical properties and microbial responses in biochar-amended soils: Mechanisms and future directions. *Agriculture Ecosystems & Environment, 206*, 46-59.

Han, Y. X., Boateng, A. A., Qi, P. X., Lima, I. M., & Chang, J. M. (2013). Heavy metal and phenol adsorptive properties of biochars from pyrolyzed switchgrass and woody biomass in correlation with surface properties. *Journal of Environmental Management, 118*, 196-204.

Han, Z. T., Sani, B., Mrozik, W., Obst, M., Beckingham, B., Karapanagioti, H. K., et al. (2015). Magnetite impregnation effects on the sorbent properties of activated carbons and biochars. *Water Research, 70*, 394-403.

Johnson, D. B., & Hallberg, K. B. (2005). Acid mine drainage remediation options: a review. *Science of the Total Environment, 338*(1-2), 3-14.

Kappler, A., Wuestner, M. L., Ruecker, A., Harter, J., Halama, M., & Behrens, S. (2014). Biochar as an Electron Shuttle between Bacteria and Fe(III) Minerals. *Environmental Science & Technology Letters, 1*(8), 339-344.

Keller, K. L., Rapp-Giles, B. J., Semkiw, E. S., Porat, I., Brown, S. D., & Wall, J. D. (2014). New Model for Electron Flow for Sulfate Reduction in Desulfovibrio alaskensis G20. *Applied and Environmental Microbiology, 80*(3), 855-868.

Kloss, S., Zehetner, F., Dellantonio, A., Hamid, R., Ottner, F., Liedtke, V., et al. (2012). Characterization of Slow Pyrolysis Biochars: Effects of Feedstocks and Pyrolysis Temperature on Biochar Properties. *Journal of Environmental Quality, 41*(4), 990-1000.

Kluepfel, L., Keiluweit, M., Kleber, M., & Sander, M. (2014). Redox Properties of Plant Biomass-Derived Black Carbon (Biochar). *Environmental Science & Technology, 48*(10), 5601-5611.

Kondo, R., Nedwell, D. B., Purdy, K. J., & Silva, S. D. (2004). Detection and enumeration of sulphate-reducing bacteria in estuarine sediments by competitive PCR. *Geomicrobiology Journal, 21*(3), 145-157.

Lapakko, K. A., and Antonson D. A. (2012). Duluth Complex Rock Dissolution and Mitigation Techniques: A summary of 35 years of DNR research. Saint Paul: Minnesota Department of Natural Resources.

Lehmann, J., Rillig, M. C., Thies, J., Masiello, C. A., Hockaday, W. C., & Crowley, D. (2011a). Biochar effects on soil biota - A review. *Soil Biology & Biochemistry, 43*(9), 1812-1836.

Lehmann, J., Rillig, M. C., Thies, J., Masiello, C. A., Hockaday, W. C., & Crowley, D. (2011b). Biochar effects on soil biota - A review. *Soil Biology & Biochemistry, 43*(9), 1812-1836.

Li, Y. C., Shao, J. G., Wang, X. H., Deng, Y., Yang, H. P., & Chen, H. P. (2014). Characterization of Modified Biochars Derived from Bamboo Pyrolysis and Their Utilization for Target Component (Furfural) Adsorption. *Energy & Fuels, 28*(8), 5119-5127.

Limousin, G., Gaudet, J. P., Charlet, L., Szenknect, S., Barthes, V., & Krimissa, M. (2007). Sorption isotherms: A review on physical bases, modeling and measurement. *Applied Geochemistry, 22*(2), 249-275.

Lovley, D. R., Coates, J. D., BluntHarris, E. L., Phillips, E. J. P., & Woodward, J. C. (1996). Humic substances as electron acceptors for microbial respiration. *Nature, 382*(6590), 445-448.

Lovley, D. R., Roden, E. E., Phillips, E. J. P., & Woodward, J. C. (1993). ENZYMATIC IRON AND URANIUM REDUCTION BY SULFATE-REDUCING BACTERIA. *Marine Geology, 113*(1-2), 41-53.

Lu, H. L., Zhang, W. H., Yang, Y. X., Huang, X. F., Wang, S. Z., & Qiu, R. L. (2012). Relative distribution of Pb2+ sorption mechanisms by sludge-derived biochar. *Water Research, 46*(3), 854-862.

Minnesota DNR. (2013). NorthMet Mining Project and Land Exchange SDEIS. Minnesota DNR.

Minnesota Pollution Control Agency. (2015). March 2015 proposed approach for Minnesota's sulfate standard to protect wild rice. MPCA.

Muyzer, G., & Stams, A. J. M. (2008). The ecology and biotechnology of sulphate-reducing bacteria. *Nature Reviews Microbiology, 6*(6), 441-454.

Nies, D. H. (1999). Microbial heavy-metal resistance. *Applied Microbiology and Biotechnology, 51*(6), 730-750.

Nomanbhay, S. M., & Palanisamy, K. (2005). Removal of heavy metal from industrial wastewater using chitosan coated oil palm shell charcoal. *Electronic Journal of Biotechnology, 8*(1), 43-53.

Nordstrom, D. K. (2011). Mine Waters: Acidic to Circumneutral. *Elements, 7*(6), 393-398.

Rapp, B. J., & Wall, J. D. (1987). GENETIC TRANSFER IN DESULFOVIBRIO-DESULFURICANS. *Proceedings of the National Academy of Sciences of the United States of America, 84*(24), 9128-9130.

Robb, G. A., & Robinson, J. D. F. (1995). ACID DRAINAGE FROM MINES. *Geographical Journal, 161*, 47-54.

Roden, E. E., Kappler, A., Bauer, I., Jiang, J., Paul, A., Stoesser, R., et al. (2010). Extracellular electron transfer through microbial reduction of solid-phase humic substances. *Nature Geoscience, 3*(6), 417-421.

Shi, L., Dong, H. L., Reguera, G., Beyenal, H., Lu, A. H., Liu, J., et al. (2016). Extracellular electron transfer mechanisms between microorganisms and minerals. *Nature Reviews Microbiology, 14*(10), 651-662.

Sun, Y. N., Gao, B., Yao, Y., Fang, J. N., Zhang, M., Zhou, Y. M., et al. (2014). Effects of feedstock type, production method, and pyrolysis temperature on biochar and hydrochar properties. *Chemical Engineering Journal, 240*, 574-578.

Tan, X. F., Liu, Y. G., Zeng, G. M., Wang, X., Hu, X. J., Gu, Y. L., et al. (2015). Application of biochar for the removal of pollutants from aqueous solutions. *Chemosphere, 125*, 70-85.

Trumm, D. (2010). Selection of active and passive treatment systems for AMDflow charts for New Zealand conditions. *New Zealand Journal of Geology and Geophysics, 53*(2-3), 195-210.

Xu, S. N., Adhikari, D., Huang, R. X., Zhang, H., Tang, Y. Z., Roden, E., et al. (2016). Biochar-Facilitated Microbial Reduction of Hematite. *Environmental Science & Technology, 50*(5), 2389-2395.

Yu, L. P., Yuan, Y., Tang, J., Wang, Y. Q., & Zhou, S. G. (2015). Biochar as an electron shuttle for reductive dechlorination of pentachlorophenol by Geobacter sulfurreducens. *Scientific Reports, 5*.